PERGAMON

Deep-Sea Research I 45 (1998) 1977–2010

DEEP-SEA RESEARCH
PART I

Abyssal recipes II: energetics of tidal and wind mixing

Walter Munk[a,*], Carl Wunsch[b]

[a] *University of California-San Diego, Scripps Inst of Oceanography, 9500 Gilman Drive, La Jolla, CA 92093-0225, USA*
[b] *Massachusetts Institute of Technology, USA*

Received 7 November 1997; received in revised form 13 April 1998; accepted 29 June 1998

Abstract

Without deep mixing, the ocean would turn, within a few thousand years, into a stagnant pool of cold salty water with equilibrium maintained locally by near-surface mixing and with very weak convectively driven surface-intensified circulation. (This result follows from Sandström's theorem for a fluid heated and cooled at the surface.) In this context we revisit the 1966 "Abyssal Recipes", which called for a diapycnal diffusivity of 10^{-4} m^2/s (1 cgs) to maintain the abyssal stratification against global upwelling associated with 25 Sverdrups of deep water formation. Subsequent microstructure measurements gave a pelagic diffusivity (away from topography) of 10^{-5} m^2/s — a low value confirmed by dye release experiments.

A new solution (without restriction to constant coefficients) leads to approximately the same values of global upwelling and diffusivity, but we reinterpret the computed diffusivity as a surrogate for a small number of concentrated sources of buoyancy flux (regions of intense mixing) from which the water masses (but not the turbulence) are exported into the ocean interior. Using the Levitus climatology we find that 2.1 TW (terawatts) are required to maintain the global abyssal density distribution against 30 Sverdrups of deep water formation.

The winds and tides are the only possible source of mechanical energy to drive the interior mixing. Tidal dissipation is known from astronomy to equal 3.7 TW (2.50 $\pm$ 0.05 TW from M_2 alone), but nearly all of this has traditionally been allocated to dissipation in the turbulent bottom boundary layers of marginal seas. However, two recent TOPEX/POSEIDON altimetric estimates combined with dynamical models suggest that 0.6–0.9 TW may be available for abyssal mixing. A recent estimate of wind-driving suggests 1 TW of additional mixing power. All values are very uncertain.

A surprising conclusion is that the equator-to-pole heat flux of 2000 TW associated with the meridional overturning circulation would not exist without the comparatively minute mechanical mixing sources. Coupled with the findings that mixing occurs at a few dominant sites, there

* Corresponding author. Fax: 001 619 534 6251; e-mail: wmunk@ucsd.edu.

0967-0637/98/$–see front matter
PII: S0967-0637(98)00070-3

is a host of questions concerning the maintenance of the present climate state, but also that of paleoclimates and their relation to detailed continental configurations, the history of the Earth–Moon system, and a possible great sensitivity to details of the wind system.

1. Introduction

The strength of the integrated meridional overturning[1] circulation (MOC), particularly its heat transport, is intimately bound up with the distribution and intensity of ocean mixing. Although this linkage has been known for many years, discussions of the MOC and ocean mixing processes have been conducted with little or no acknowledgement of their connection. One can trace the beginnings of the discussion to Sandström's (1908) paper and a rejoinder by Jeffreys (1925). Sandström concluded that an ocean heated and cooled at the same geopotential, or heated at a higher geopotential than it is cooled (the actual case), has *in a steady state* a very weak convectively driven circulation, one which is significant only in a thin upper layer. The abyss of such an ocean would be of essentially uniform density at the value set by the properties of the downward part of the convective cell. Jeffreys (1925) pointed out that "Sandström's theorem," as it is sometimes known, would fail if there is turbulent mixing capable of carrying the warm fluid to a lower geopotential than in the region of initial convection.

Neither Sandström nor Jeffreys knew of the existence of the vigorous convective motions in the ocean, and so their discussion was abstract. In particular, Jeffreys had no reason to pursue the question of the energy source for the mechanical mixing. More recent discussions by Faller (1968), Colin de Verdiere (1993), and Huang (1998a) have made the connection between large-scale convective motions and mechanical mixing.

We need a rough estimate of global deep water formation rate. The very definition of bottom water formation rates is vague owing to the importance of entrainment in forming water mass properties. Killworth (1983) did not give a total value in his review of deep convection. The Munk (1966) model was consistent with about 25 Sv (1 Sv = 10^6 m^3/s). Stommel and Arons (1960) estimated values ranging from 15 to 90 Sv, expressing a weak preference for values of around 30–35 Sv. For present purposes, the value needed is the upwelling across a fixed abyssal depth within our region of integration. Macdonald and Wunsch (1996) estimated about 29 Sv net upwelling across the 3.5° isotherm. We will thus use a nominal value of 30 Sv, well within the very broad limits that have been recently estimated (e.g., Whitworth et al. 1998).

[1] We prefer "meridional overturning" to the more traditional "thermohaline" or "convective overturning" designations, as these imply a buoyancy flux for the primary power source.

If this fluid is not mixed back to surface properties, the abyssal ocean would simply fill up with fluid at the temperature and density of the deepest convecting element (Baines and Turner, 1969). Samelson and Vallis (1997) discuss a model with very small vertical mixing, which does precisely that. A 30 Sv source would take about 3000 yr to fill the ocean.

The meridional oceanic heat flux is crucial in determining the climate state. Macdonald and Wunsch (1996) estimate this flux to be of the order of 2×10^{15} W (2 PW), a thousand times the tidal dissipation. The enormous heat exchange between ocean and atmosphere would suggest that the buoyancy forces drive the MOC. But, as Sandström pointed out, the ocean is not a heat engine in the same sense as the atmosphere (e.g. Peixoto and Oort, 1992). Energy available from buoyancy forcing (including fresh water exchange) appears to be much too small to drive the MOC (Faller, 1968; Oort et al., 1994). Viewed as a heat engine, the ocean circulation is extraordinarily inefficient. Viewed as a mechanically driven system, it is a remarkably effective transporter of heat energy.

This raises some fundamental questions. What is the dependence of the MOC on the sources of mechanical energy available for mixing the abyssal ocean? What determines the associated heat flux? What are the climate implications? We note that fluctuations in the strength of the MOC have, in recent discussions, become a kind of *deus ex machina*[2] for many postulated climate changes. Any serious attempt to forecast future climate states requires an understanding of the present state. In this paper, we set out some of what appear to be the salient questions, but raise many more questions than we are able to answer.

How and where fluid returns to the surface has remained obscure to this day. Munk (1966) explored the consequences of a *uniform* upwelling over the entire abyssal ocean. He assumed a one-dimensional advection/diffusion balance of the form

$$w \frac{\partial \rho}{\partial z} = \kappa \frac{\partial^2 \rho}{\partial z^2}, \tag{1.1}$$

with constant w and κ. This balance was assumed to apply *point-wise*, and when fit to density and radiocarbon data from the central Pacific Ocean led to values of the order $w \approx 0.7 \times 10^{-7}$ m/s, $\kappa \approx 10^{-4}$ m^2/s ($=1$ cm^2/s). The value of w is, neatly enough, that required to balance global bottom water formation at a rate of roughly 25 Sv. In the intervening 30 yr, model (1.1) became much used, particularly by the geochemical community, which was attracted by its simplicity. Eq. (1.1) also appears as the vertical balance in one class of solutions to the so-called thermocline equations (see Stommel and Webster, 1962).

Supposing that balances such as Eq. (1.1) (with the vertical coordinate z re-interpreted as normal to the isopycnals) describe at least in part the way in which both bottom and intermediate waters return toward the surface. This implies that work must be done to carry the fluid across the stable stratification, whether or not the upwelling w is confined to restricted areas. *One immediate inference is that the strength*

[2] Referring to Greek drama where a god pops out of a box to resolve all plot problems.

of the MOC and associated heat flux may well be primarily determined not by the high-latitude buoyancy forcing, but by the power available to return the fluid to the surface layers.

The remainder of this paper is devoted primarily to two tasks: first, we make a new estimate of the rate at which the abyssal ocean mixes and of the power required to support the mixing. Then we explore possible power sources: (a) winds, (b) surface buoyancy forcing, (c) tides, and (d) geothermal heating through the seafloor. We find (b) and (d) to be relatively unimportant. Power available from winds and tides[3] appears (surprisingly) to be comparable and of the magnitude (order 2 TW) required to sustain abyssal mixing (a conclusion subject to major revision). Much of the remainder of this paper explores the possibility of tides as an important, even dominant, element in mixing the abyssal ocean. Recent progress in tidal modeling has made such estimates possible (but just barely). To many readers, the proposal that the Moon plays a major role in the general circulation will border on the lunatic. In all of this, there remains the question whether *any* one-dimensional treatment can capture elements of a three-dimensional ocean circulation. The answer must depend upon whether the analysis contributes to the understanding of ocean processes.

2. Dichotomy of diffusivities

A number of developments have undermined the simple picture of the gross oceanic mixing described in Munk (1966). These range from recognition that the value $\kappa = 10^{-4}$ m^2/s (1 cgs unit) is an accident of an ill-conditioned set of equations (see Olbers and Wenzel, 1989), to the more fundamental result that direct measurements produced values an order of magnitude lower than 10^{-4} m^2/s. In the discussion below, we will show that a global average value near 10^{-4} m^2/s (if properly interpreted) is still required to explain the gross oceanic stratification.

The discrepancy between the diffusivity κ_{AS} inferred from the abyssal stratification and the value κ_{PE} obtained from direct pelagic measurements (away from topography) has been known since the 1970s. Mixing takes place at scales of 1 mm to 1 m, where turbulence generates property gradients that are irreversibly removed by molecular diffusion. The small scale of the mixing processes makes quantitative assessment very difficult. Measurements pioneered by C. Cox and his collaborators (Osborn and Cox, 1972; Gregg, 1989) have led over time to a "pelagic diffusivity" of $\kappa = \kappa_{PE} \approx 10^{-5}$ m^2/s, i.e. about 1/10 the κ_{AS} value (but still two orders of magnitude above the molecular value for thermal diffusivity).

The determination of κ from microstructure measurements is based on some plausible but unproven assumptions (see Davis, 1994a, b). Stigebrandt (1979) reported a tracer release experiment in Oslofjord in the summer of 1977 that yielded

[3] Stigebrandt (1979) long ago demonstrated that the circulation in fjords is driven by the breaking of internal tides generated at the sills (Stigebrandt and Aure, 1989). Sjöberg and Stigebrandt (1992) have extended these concepts to the global mixing problem. There are many similarities (and differences) in their treatment and the discussion given here.

a coefficient of vertical diffusion of about 10% of that determined from the density structure. But it was only with the general confirmation by direct dye release in the open ocean (e.g. Ledwell et al., 1993) that a wider community has come to accept the low interior value of the mixing coefficient. Furthermore, microstructure measuring technology has developed to the point that one could directly determine dissipation rates (Kunze and Sanford, 1996; Lueck and Mudge, 1997).

Greatly enhanced values of κ, up to 10^{-1} m^2/s, have been found in some boundary regions (e.g., Polzin et al., 1995, 1997), and it is a reasonable hypothesis that the actual extremes (possibly in canyons, see for example, Hotchkiss and Wunsch (1982) and Hickey (1997)) have not yet been discovered. Observations generally showed that the elevated mixing rates settle back to the pelagic $\kappa_{PE} = 10^{-5}$ m^2/s values a few hundred meters above and a few km away from topographic features.

Given the dichotomy of diffusivities, two points of view have been adopted. The "conventional" view ignores the dichotomy, and assumes quasi-uniform mixing everywhere in the ocean at a rate roughly proportional to $\kappa\,\partial^2\rho/\partial z^2$, with either constant κ, or one varying only in the vertical direction. This mechanism is used in almost all oceanic general circulation models (GCM).

The second view is that the ocean mixes primarily at its boundaries—a possibility already suggested by Munk (1966). This proposal has been followed by a small exploratory literature of both theory and observation (e.g. Schiff, 1966; Wunsch, 1970, 1972; Armi, 1978; Garrett, 1979; Garrett and Gilbert, 1988; Eriksen, 1985; Kunze and Sanford, 1996). Armi (1978) has found benthic boundary layers of order 100 m thickness with remarkably uniform (to within 2 millidegrees) potential temperature. In his model of ocean mixing these benthic boundary layers are intermittently swept into the interior and then re-form. In Armi's words, the two processes, vertical mixing forming these layers and their subsequent lateral advection, have, in various ocean circulation models, been "... parametrically disguised as a vertical eddy diffusivity."

Mixing across isopycnals requires power; our hypothesis is that the power required for a buoyancy flux associated with $\kappa_{AS} = 10^{-4}$ m^2/s and distributed over the entire ocean area is the same as if concentrated mixing associated with (say) 10^{-2} m^2/s occurred over only 1% of the oceans.

In this sense it is not fruitful to think in terms of a dichotomy between a κ_{PE} of 10^{-5} m^2/s and a κ_{AS} of 10^{-4} m^2/s. The former is properly interpreted as a measure of turbulent diffusion *distributed* over nearly all of the ocean area. The latter is interpreted as a surrogate for a small number of concentrated source regions of buoyancy flux from which the water masses (but not the turbulence) are exported into the ocean exterior. Comparing κ_{PE} and κ_{AS} is like comparing applesauce and oranges.

3. The one-dimensional flux balance

We now revisit Munk's (1966) paper, but with the point of view that the balance of Eq. (1.1) refers to *spatially averaged* properties of an oceanic interior in which the vertical mixing is weak (but not zero) and of boundary regions with much enhanced

mixing. We are concerned with the abyssal density distribution in temperate latitudes Fig. 1. Isopycnals that outcrop between 40°S and 50°N, say, penetrate at mid-latitudes to about 1 km depth, so somewhat arbitrarily we take the upper boundary of validity to Eq. (1.1) at 1 km. That is, we focus on the circulation in the abyssal ocean where the isopycnals generally outcrop only in the convective regions themselves. The lower limit is taken at 4 km, above the depth of densest water.

We begin with a general steady advective/diffusive balance, for potential temperature θ, and salinity S:

$$u\frac{\partial\theta}{\partial x}+v\frac{\partial\theta}{\partial y}+w\frac{\partial\theta}{\partial z}=\frac{\partial}{\partial z}\left(\kappa(z)\frac{\partial\theta}{\partial z}\right), \tag{3.1}$$

$$u\frac{\partial S}{\partial x}+v\frac{\partial S}{\partial y}+w\frac{\partial S}{\partial z}=\frac{\partial}{\partial z}\left(\kappa(z)\frac{\partial S}{\partial z}\right) \tag{3.2}$$

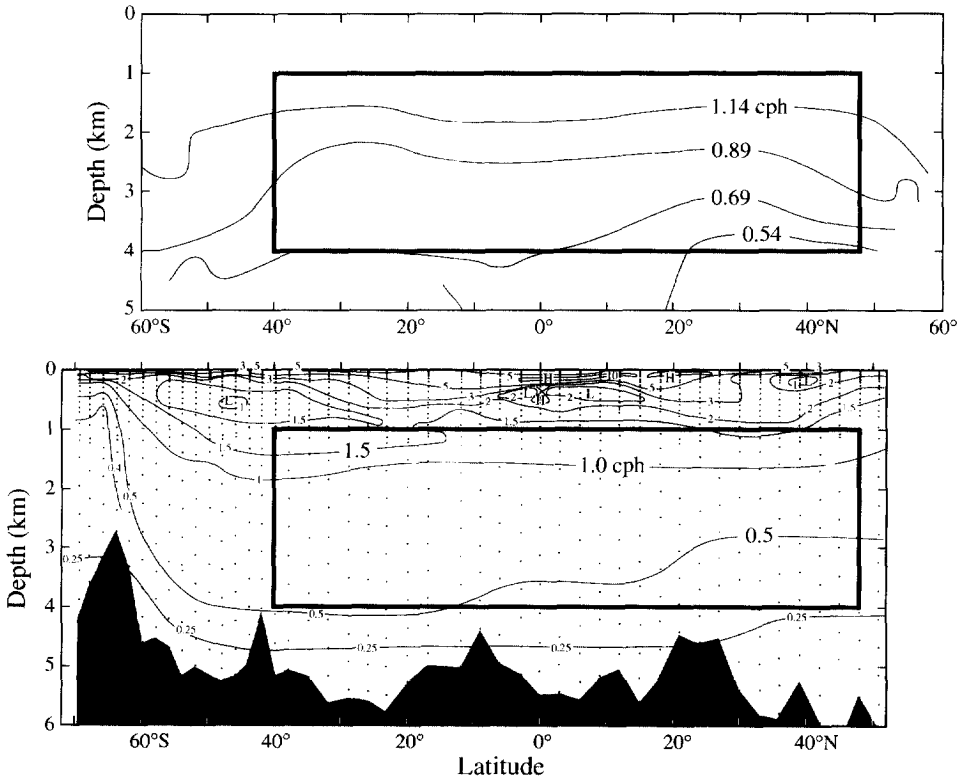

Fig. 1. Contours of buoyancy frequency as function of latitude. TOP: global average of 10° squares (based on Levitus et al., 1994; Levitus and Boyer, 1994). BOTTOM: Central Pacific (1700 W) (Munk et al., 1995). Contours are relatively uniform within the "abyssal ocean", defined as extending from 40°S to 48°N between 1 and 4 km depth, as shown.

and mass conservation

$$\frac{\partial u}{\partial x}+\frac{\partial v}{\partial y}+\frac{\partial w}{\partial z}=0.$$

The same eddy diffusivity, κ, applies to temperature and salt. If the diffusion were associated with molecular processes, the distributions of temperature and salinity would be sharply different, which is not the case (Munk, 1966); furthermore, the diffusive flux would be associated with the in situ temperature gradient (the final diffusive state is isothermal, not adiabatic).

The equations are integrated[4] in x, y over an ocean volume between 1 and 4 km that includes both the low mixing interior and regions assumed to exhibit greatly enhanced mixing, such as near western and eastern boundaries, mid-ocean ridges, seamounts and islands. Regions poleward of 48°N and 40°S, which show enhanced mixing, are excluded; these are also the source regions of convective injection of fluid into the interior.

We assume w is not correlated with θ, S (the turbulent fluxes $\langle w\theta'\rangle$ and $\langle wS'\rangle$ are parameterized as a diffusivity), and so in the basin average

$$\langle w\theta\rangle\cong\langle w\rangle\langle\theta\rangle,\quad \langle wS\rangle\cong\langle w\rangle\langle S\rangle.$$

The result of the x, y-integration is then

$$\frac{\mathrm{d}}{\mathrm{d}z}\left(w\theta-\kappa\frac{\mathrm{d}\theta}{\mathrm{d}z}\right)=A^{-1}q(z)\,\theta(z), \tag{3.3}$$

$$\frac{\mathrm{d}}{\mathrm{d}z}\left(wS-\kappa\frac{\mathrm{d}S}{\mathrm{d}z}\right)=A^{-1}q(z)\,S(z). \tag{3.4}$$

Here $\mathrm{d}\theta/\mathrm{d}z$ is the potential (in situ minus adiabatic) temperature gradient, and $q(z)$ represents the injection of water volume, with corresponding temperature and salinity properties, at the edges of the region of integration (the regions of strong mixing, convection, and entrainment are visualized as setting these properties prior to entry). A is the area of integration. All parameters are now basin averages $\langle f(x,y,z)\rangle_{xy}=f(z)$, and the averaging bracket is dropped to simplify the notation.

For a linear equation of state, $\rho=-a\theta+bS$, multiplying the first equation by $-a$ and the second by b, and adding, gives

$$\frac{\mathrm{d}}{\mathrm{d}z}\left(w\rho-\kappa\frac{\mathrm{d}\rho}{\mathrm{d}z}\right)=A^{-1}q(z)\rho(z). \tag{3.5}$$

[4] We recognize that the analysis should be carried out in isopycnal or neutral surface coordinates. But we wish to retain the immediate connection to the original Abyssal Recipes paper and note that the results are nearly the same (Szoeke and Bennett, 1993), given the small isopycnal slopes in the abyssal ocean interior. The poor data coverage and weak stratification in much of the abyssal ocean often renders highly unstable calculations of isopycnal depths.

Substitution of $q = A\,\mathrm{d}w/\mathrm{d}z$ leads to a first-order differential equation in the potential density gradient $\rho' = \mathrm{d}\rho/\mathrm{d}z$:

$$\frac{\mathrm{d}\rho'}{\mathrm{d}z} - \alpha\rho' = 0, \quad \alpha(z) = \frac{w - \kappa'}{\kappa} \tag{3.6}$$

where $\kappa' = \mathrm{d}\kappa/\mathrm{d}z$. This same equation was discussed by Armi (1979).

Theory (e.g. Pedlosky, 1996) predicts an Ekman-driven equatorial upwelling of isopycnals and vertical velocities (downward in the subtropical gyre, upward in the subpolar gyre) of order 10^{-6} m/s, as compared to $w = 10^{-7}$ m/s from Abyssal Recipes. Such latitude-dependent features are largely confined to the upper 1 km, and it appears that the vertical density gradients in the abyssal domain are insensitive to latitude (Fig. 1).

Eq. (3.6) has a simple, exact solution:

$$\rho'(z) = \rho'_0\,\mathrm{e}^{I(z)}, \quad I(z) = \int_0^z \alpha(\zeta)\,\mathrm{d}\zeta \tag{3.7}$$

$$\rho(z) = \rho_0 + \rho'_0 \int_0^z \mathrm{e}^{I(\eta)}\,\mathrm{d}\eta \tag{3.8}$$

where $\rho_0 = \rho(0)$ and $\rho'_0 = \rho'(0)$ are integration constants. For the case of a depth-independent $\alpha = w/\kappa$ (as in Munk, 1966) the solution is $\rho' = \rho'_0\,\mathrm{e}^{\alpha z}$, which, as we shall see, gives an abysmal fit to the abyssal density gradients. There is no point to such further approximation.

The "stratification function"

$$I(z) = \ln[\rho'(z)/\rho'_0] = 2\ln[N(z)/N_0] \tag{3.9}$$

is a convenient starting point in estimating the depth-dependent upwelling and diffusivity from the measured density distribution (Fig. 2). The procedure followed here is to estimate $I(z)$ from the Levitus climatology, make some guess as to $w(z)$, and then solve

$$\alpha(z) = \mathrm{d}I/\mathrm{d}z = (w - \kappa')/\kappa \tag{3.10}$$

for κ. We have a differential equation

$$\mathrm{d}\kappa/\mathrm{d}z + \alpha(z)\,\kappa = w(z) \tag{3.11}$$

with the general solution

$$\kappa(z) = \mathrm{e}^{-I(z)}\left[\kappa_0 + \int_{z_0}^z w(\zeta)\,\mathrm{e}^{I(\zeta)}\,\mathrm{d}\zeta\right] \tag{3.12}$$

where $\kappa_0 = \kappa(z_0)$ is an undetermined constant. Eq. (3.11) specifies that κ will change with depth so as to approach its "equilibrium" value w/α at a rate proportional to $(w/\alpha) - \kappa$. Within a layer of constant α and w, the solution can be written

$$\kappa(z) = (w/\alpha) + (\kappa_0 - w/\alpha)\exp(-\alpha z) \tag{3.13}$$

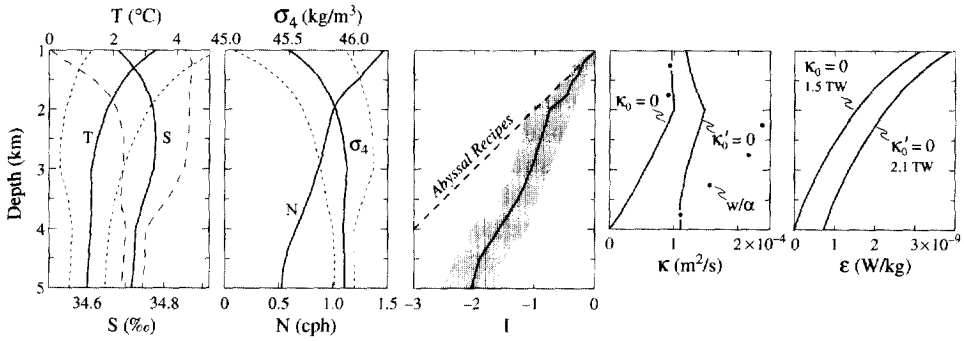

Fig. 2. Procedure for estimating diffusivity $\kappa_{AS}(z)$ and energy dissipation $\varepsilon_{AS}(z)$ required for the maintenance of abyssal stratification. The left two panels show globally averaged profiles of temperature, salinity, density (in σ_4 units), and buoyancy frequency N based on the Levitus Atlas, with error limits as indicated. A lot of scatter occurs in the climatology at depth, and a substantial number of the Levitus profiles are statically unstable (see Jackett and McDougall, 1995). These stations were omitted from the average. The "stratification function" $I(z) = 2\log(N/N_0)$ shown in the third panel (with N_0 taken at 1 km depth) permits the evaluation of $\alpha = dI/dz$. (Abyssal Recipes took a constant α, as shown). The diffusivity $\kappa_{AS}(z)$ and dissipation $\varepsilon(z)$ are derived from $\alpha(z)$ for the two cases $\kappa = 0$ and $\kappa' = 0$ at the lower boundary, under the assumption of a constant $w = 0.7 \times 10^{-7}$ m/s corresponding to 25 Sv of bottom water formation. The global dissipations of 1.3 and 1.9 TW, respectively, are computed from Eq. (3.15) for a mixing ratio $\gamma = 0.2$.

where $\kappa_0 = \kappa(0)$ at the lower layer boundary. The case $\kappa_0 = w/\alpha$ and hence $\kappa(z) = (w/\alpha) =$ constant is a special case. If $\alpha(z) = dI/dz \approx 0$, the implied $\kappa(z)$ becomes very large—this is a problem in the South Pacific (Section 6).

What determines the overall vertical density distribution in the oceans? Why is the buoyancy frequency $N(-1$ km) near 1 cycle per hour (cph) and not 10 cph? We take the view that the density distribution is controlled jointly by the injection of water masses at a few selected sites (determining the global water formation rate $q(z)$) and intensive turbulent mixing in some areas along the ocean boundaries (determining the global $\kappa_{AS}(z)$). The hypothesis can be tested for a known $q(z)$ and $\kappa(z)$ by solving for the stratification $\rho'(z)$ (or equivalently $N(z)$) by simple integration and for $\rho(z)$ (if required) by a second integration. But this is not a feasible procedure.[5] We know something about $\rho(z)$, a little about $q(z)$, and almost nothing about $\kappa(z)$. An operational procedure is to start with the measured density distribution and infer $\kappa(z)$.[6]

[5] Even if $\kappa(z)$ were known and $\alpha(z)$ determined from the density distribution, the source function $q(z) \sim w' \sim \alpha' \sim I'' \sim \rho'''(z)$ is proportional to the third derivative of the density distribution. It is disturbing that with all the hydrographic measurements it is still impossible to estimate higher derivatives in the global density profile.

[6] Sjöberg and Stigebrandt (1992) do in fact estimate the global tidal dissipation over a steppy ocean bottom and infer $\kappa(x, y, z)$ from an empirical law based on their extrapolation from Oslofjord. The procedure yields estimates of global upwelling and dissipation of the same order as those found here.

3.1. Inference from the global density distribution

We apply the foregoing formulae to the climatology compiled by Levitus and Boyer (1994) and Levitus et al. (1994). The distribution of deep stations remains surprisingly sparse (Levitus et al. Fig. A20), even after all the years of global exploration, and so our estimates are uncertain. The estimation follows the procedure $T, S \to \rho(z) \to N(z) \to I(z) \to \kappa(z) \to \varepsilon$ as illustrated in Fig. 2 and Appendix A (expressions for the dissipation ε are derived below). We have taken a constant slope $\alpha = \delta I/\delta z$ within each of six 500 m thick abyssal layers, -4––3.5 km, ..., -1.5 km––1 km. The dashed curve in panel 3 of Fig. 2 shows the overall constant α adopted by Munk (1966).

Panel 4 is drawn for a constant $w = 0.8 \times 10^{-7}$ m/s corresponding to 30 Sv injected beneath 4 km and no further injection aloft. The dots show values of w/α in each of the six layers. κ is subject to an undetermined constant of integration κ_0. We have taken two extreme cases. The first case assumes $\kappa_0 = 0$ at the lower boundary of the abyssal ocean; the second case assumes $\kappa_0' = 0$, and so $\kappa_0 = w/\alpha$ in the lowest layer. (Subsequent calculations are limited to the second case.) The average value of κ_{AS} is of the order 10^{-4} m^2/s — which is the value used in Abyssal Recipes to maintain the abyssal stratification. Overall values of this magnitude were found by Hogg et al. (1982) and Hogg (personal communication, 1998) by consideration of the temperature balance for Antarctic Bottom Water in the Brazil Basin.

3.2. Dissipation of energy

We now estimate the power required to achieve the postulated diffusion. In the open ocean, away from topography, the internal wave field is the only serious candidate for vertical mixing. Observations indicate that in the deep sea the internal wave intensities are near values indicative of shear instability (Alford and Pinkel, 1998). Shear instability leads to a conversion of a portion of the turbulent kinetic energy into potential energy through vertical buoyancy flux. Only a fraction, the "mixing efficiency" γ, of the dissipation of turbulent energy goes into the production of potential energy, $\varepsilon_p = \gamma\varepsilon$; the remaining fraction $(1 - \gamma)\varepsilon$ goes into heat.[7]

The mixing efficiency is related to the flux Richardson number Ri_f according to $\gamma = Ri_f/(1 - Ri_f)$. We adopt Osborn's (1980) upper bound $\gamma = 0.2$. (The widely used value $Ri_f = 1/5$ corresponds to $\gamma = 1/4$.) The rate of work done against gravity in a stable stratified fluid is written

$$\varepsilon_p = \gamma\varepsilon = \kappa(g/\rho)(-\mathrm{d}\rho/\mathrm{d}z) = \kappa N^2 \quad \mathrm{W/kg(or\ m^2/s^3)}. \tag{3.14}$$

Eq. (3.14) serves as a definition of the "diapycnal diffusivity" κ. Further development now takes two quite separate directions.

[7] The density change $\mathrm{d}\rho/\mathrm{d}t$ associated with the 80% of energy going into heat is of the order of 10^{-7} of the term $w\,\mathrm{d}\rho/\mathrm{d}z$ associated with upwelling, and thus utterly negligible. Stirring a cup of coffee will change its stratification without appreciably heating the coffee.

3.3. Pelagic dissipation

We define "pelagic dissipation" to occur in the open sea, away from topography, consistent with κ_{PE}. ("Abyssal dissipation" includes both boundary and pelagic processes.) Open sea measurements show that the dissipation rate, $\varepsilon(z)$, is proportional to $N^2(z)$ over a wide range of conditions (Gregg, 1989; Polzin et al., 1995; Kunze and Sanford, 1996). Assuming the rule to apply universally, this proportionality makes κ_{PE} a useful measure of pelagic turbulent dissipation. Integrating $\rho\varepsilon(z) = \rho\gamma^{-1}\varepsilon_p(z)$ with depth and multiplying by A gives the global dissipation

$$D_{PE} = A\int \rho\,\varepsilon\,dz = A\,\rho\,\gamma^{-1}\,\kappa_{PE}\int N^2\,dz = g\,\gamma^{-1}\,\kappa_{PE}\,A\,\Delta\rho\,W \tag{3.15}$$

which equals 0.2 TW for the pelagic ocean using $\gamma = 0.2$, $\kappa_{PE} = 10^{-5}\ m^2/s$, $A = 3.6\times10^{14}\ m^2$, $\Delta\rho = 10^{-3}\rho = 1\ kg/m^3$.

3.4. Abyssal stratification

Maintenance of abyssal stratification against an upwelling velocity $w(z)$ determines the profiles for $\rho'(z)$ and $\kappa(z)$ according to Eqs. (3.7) and (3.12) and yields

$$\varepsilon_p(z) = \kappa_{AS}(z)\,N^2(z) = N_0^2\left(\kappa_0 + \int_{z_0}^{z} w(\zeta)\,e^{I(\zeta)}\,d\zeta\right)W/kg. \tag{3.16}$$

Integrating $\rho\,\varepsilon(z) = \rho\,\gamma^{-1}\,\varepsilon_p(z)$ with depth and multiplying by the ocean area A gives the global dissipation.[8] The last panel in Fig. 2 gives the result for the global ocean. The inferred abyssal dissipation is $D_{AS} = 2.1$ TW.

For illustration, we temporarily revert to the case of constant w and κ. The global total dissipation is again given by Eq. (3.15), but with $\kappa_{PE}\,A$ replaced by $\kappa_{AS}\,A = \iint\kappa\,dA$, with the integration performed over the turbulent mixing regions. Set $h = \alpha^{-1} = \kappa_{AS}/w$ as the density scale height (the buoyancy frequency scale height is $2h$). We can write $\kappa_{AS} = wh = (Q/A)h$, so that

$$D_{AS} = g\,\gamma^{-1}\,\Delta\rho\,Q\,h\,W \tag{3.17}$$

relates D_{AS}, the energy required for maintaining abyssal stratification, to Q, the global rate of formation of bottom water. We presume that the density contrast $\Delta\rho$ is determined by the equations of state of sea water, the physics of ice formation, and the surface radiation balance, so that the ocean stratification scale (a single parameter h for this special case) is determined by Eq. (3.17), given the global dissipation D_{AS} and bottom water formation Q. Taking $D_{AS} = 2$ TW, $\gamma = 0.2$, $Q = 30$ Sv, and $\Delta\rho = 1\ kg/m^3$ yields $h = 1300$ m (a high value but of the right order of magnitude). More generally, with a given global dissipation *density* $d(z)$ W/m and volume influx

[8] We continue to use the condition $\kappa'(0) = 0$; the lowest dissipation corresponds to $\kappa_0 = 0$.

$q(z)$ m^2/s, both per unit depth, the density gradient profile $\rho'(z)$ is determined by

$$\frac{d\rho'}{dz} = \frac{\gamma\, d(z)}{gQ(z)}, \quad Q(z) = \int_{z_0}^{z} q(z)\, dz. \tag{3.18}$$

We adopt the view that the density field will adjust to the overall global (or ocean basin scale) buoyancy flux and resulting water mass formation, depending only weakly on the geographic distribution of concentrated centers of mixing and water mass formation.

4. A model for lateral homogenization

We now explore in a primitive way[9] the interior consequences of the proposal that the ocean mixes primarily at its boundaries. To account for the observed distribution requires that temperature and salinity characteristics so acquired (but not turbulence) are readily exported along isopycnal (more correctly along neutral) surfaces into the deep oceanic interior, where $\kappa = \kappa_{PE} \ll \kappa_{AS}$. To quantify somewhat this concept of lateral homogenization, the balance in Eq. (1.1) between vertical diffusion and vertical advection is extended to include horizontal advection:

$$\kappa_{PE} \frac{\partial^2 \rho}{\partial z^2} - w \frac{\partial \rho}{\partial z} - u \frac{\partial \rho}{\partial x} = 0. \tag{4.1}$$

At the lateral boundary $x = 0$, the density distribution is taken as $\rho(x, z) = \rho(0, z)$ characteristic of $\kappa_{AS} = 10^{-4}$ m^2/s, whereas within the model domain $x > 0$ the diffusivity is κ_{PE} (the intense mixing zone having been conveniently exiled to $x < 0$). For large positive x the density approaches $\rho(\infty, z)$ associated with the lower diffusivity $\kappa_{PE} = 10^{-5}$ m^2/s. In the absence of any turbulent mixing the cold deep water would extend to within 1 m of the surface, consistent with the molecular thermal conductivity of 10^{-7} m^2/s.

The solution is cumbersome, and the detailed discussion has been placed into Appendix B. For $u = 0$ we have the previous solution of a profile with 0.1 km scale depth associated with the pelagic diffusivity $\kappa_{PE} = 10^{-5}$ m^2/s (Fig. 3); this is the solution to Eq. (4.1) as $x \to \infty$. On the other hand, when $u \to \infty$ the entire ocean basin has a profile with a 1 km scale depth associated with $\kappa_{AS} = 10^{-4}$ m^2/s imposed at $x = 0$. For a characteristic basin width of 10,000 km, we find that the solution approaches the former state for $u < 0.1$ mm/s, and the latter state for $u > 1$ mm/s. Because mesoscale velocities are typically well above 1 mm/s, the inference is that lateral advection and diffusion are adequate for horizontal homogenization of

[9] Marotzke (1997) explores the large-scale circulation consequences of boundary mixing in a GCM.

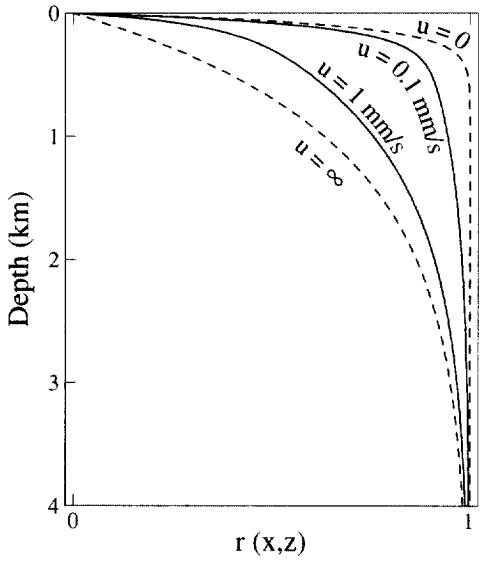

Fig. 3. For a horizontal velocity $u = \infty$, the entire ocean basin has the density profile imposed at the boundary $x = 0$, with a scale depth of 1 km (corresponding to $\kappa_{AS} = 10^{-4}$ m^2/s). For $u = 0$, the entire ocean basin has a density profile with 0.1 km depth scale associated with the pelagic diffusivity $\kappa_{PE} = 10^{-5}$ m^2/s. For $u = 1$ mm/s, the profile averaged over 10,000 km range (representing the scale of ocean basins) is close to the 1 km scale depth (as observed), for $u = 0.1$ mm/s it is close to the 0.1 km scale depth. We interpret this result as suggesting that water masses from high mixing regions at the ocean boundaries are readily advected into the interior.

ocean basins within the time constant of the vertical mixing and diffusion balance. The model of a constant penetration velocity u is, of course, totally unrealistic. (McDougall (1989) considers flows into and out of multiple ocean boundary layers.) The solution is dramatically different for negative w (Fig. 7). Downward advection and downward diffusion can no longer provide a balance, and the ocean fills laterally with light surface water. The asymmetry between upwelling and downwelling has been remarked upon by Pedlosky (1979, pp. 420–422). The problem of downwelling has some interesting geophysical implications (Appendix C).

For later reference, we remark that estimates of vertical velocity from isopycnal inclinations depend upon the assumed values of diffusivity. Isopycnals $z(x)$ have typical inclinations (Eq. (B. 16)).

$$\frac{dz}{dx} = \frac{w}{u}\left(1 - \frac{\kappa_{PE}}{\kappa_{AS}}\right). \tag{4.2}$$

For the purely advected case, $\kappa_{PE} = 0$ and $dz/dx = w/u$. For the case $\kappa_{PE} = \kappa_{AS}$, there is no x-dependence, and the isopycnals are horizontal, $dz/dx = 0$. A vertical velocity w^* inferred from the isopycnals under the assumption $\kappa_{PE} = 0$ differs from the "true"

value according to

$$w^* = w(1 - \kappa_{PE}/\kappa_{AS}). \tag{4.3}$$

5. Tidal dissipation

With a crude estimate of 2 TW for the power required to mix the abyssal ocean, we now examine the possibility that some of it is of tidal origin. Fig. 4 gives a schematic presentation of the proposed flux of tidal energy. The fraction, 2.5 TW, associated with M_2 dissipation is very well determined from astronomical measurements;[10] the total (semidiurnal plus diurnal) lunar contribution is estimated at 3.2 TW, and the total power available from Moon and Sun at 3.7 TW.[11] After allowing for a relatively small dissipation in the atmosphere and the solid Earth, 3.5 TW remain to be dissipated in the ocean. This would be adequate for carrying the entire load of ocean abyssal mixing. The amount is tiny compared to the solar radiation of 175,000 TW received by the earth, the equator-to-pole ocean heat-flow of 2000 TW, and even small compared to heat flow of 30 TW from the earth's interior.[12] Yet the tides appear to be a significant factor in the ocean circulation.

5.1. Bottom boundary layer (BBL)

Since Taylor's (1919) estimate of tidal dissipation, d, in the Irish Sea using

$$d = C_D \rho \langle u_{\text{tidal}}^3 \rangle \text{ W/m}^2, \quad C_D \approx 0.0025 \tag{5.1}$$

and Jeffrey's (1920) first global budget, it has been widely assumed that the turbulent bottom boundary layers (BBL) in the shallow seas completely dominate the dissipative budget. Typical tidal currents are of the order of 1 cm/s in the deep sea,[13] and of 1 knot $\approx$50 cm/s in shallow marginal seas. The cubic dependence of dissipation on tidal current velocity leads to the conclusion that 99% of the ocean accounts for less than 1% of the dissipation.

---

[10] Independent estimates come from ancient eclipses, from modern measurements of the length of day and month, and the tidal perturbation of artificial satellite orbits. The most precise information now comes from lunar laser ranging using the retroreflectors placed on the Moon in 1969 during the Apollo mission (Dickey et al., 1994). The semimajor axis of the Moon's orbit is increasing at a rate 3.82 ± 0.07 cm/yr. The secular acceleration of the orbit is deduced as -22.2 ± 0.6 and -4.0 ± 0.4 arcsec/century^2 associated with semidiurnal and diurnal tides, respectively.

[11] The totals are not independent because of the nonlinear interaction associated with quadratic bottom friction (e.g. Le Provost and Lyard, 1997).

[12] Tidal dissipation is comparable to the 3.5 TW of global electric generating capacity projected for 2004.

[13] Velocities associated with mesoscale circulation (which had not been discovered in Jeffreys's day) generally exceed tidal currents by a considerable margin.

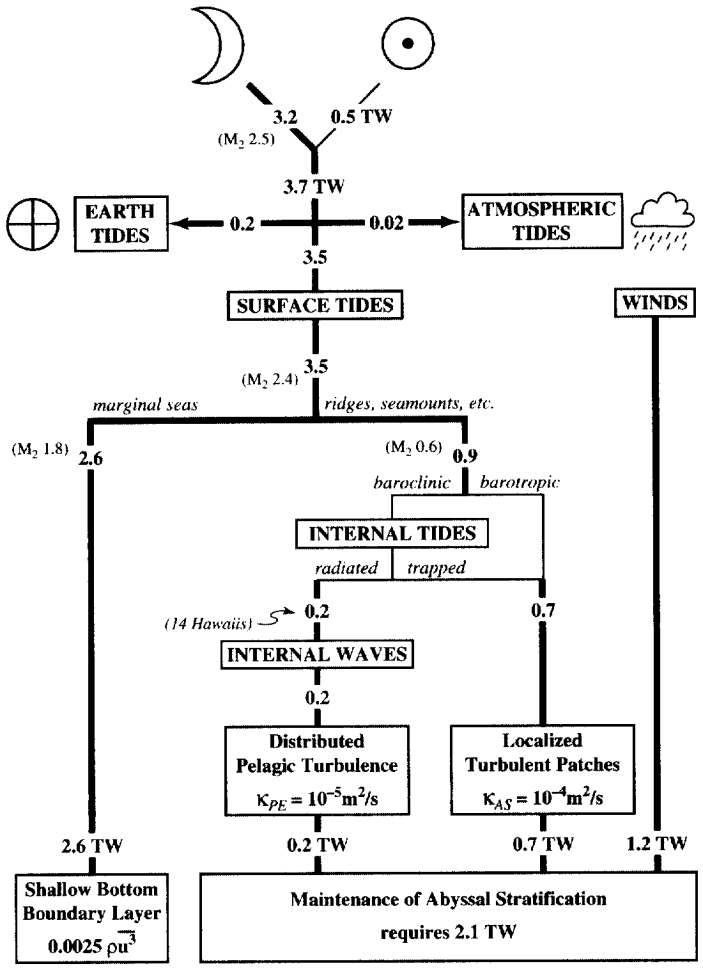

Fig. 4. An impressionistic budget of tidal energy flux. The traditional sink is in the bottom boundary layer (BBL) of marginal seas. Preliminary results from Egbert (1997) based on TOPEX/-POSEIDON altimetry suggest that 0.9 TW (including 0.6 TW of M_2 energy) are scattered at open ocean ridges and seamounts. Light lines represent speculation with no observational support. "14 Hawaiis" refers to an attempted global extrapolation of surface to internal tide scattering measured at Hawaii, resulting in 0.2 TW available for internal wave generation. The wind energy input is estimated from Wunsch (1998), to which we have added 0.2 TW to balance the energy budget. This extra energy is identified as wind-generated internal waves — radiating into the abyss and contributing to mixing processes.

The conclusion that BBL dissipation accounts for nearly all of tidal dissipation has been the accepted view since Taylor's early work. But there are many uncertainties; we note that when the astronomical estimates for the total dissipation fluctuated over the years by a factor of two before settling down to the present value, the estimated BBL dissipation kept up with the fluctuation (see Munk (1997) for a brief history). The drag

coefficient (usually set to 0.0025) is not a universal constant; direct measurements within a one cm thick viscous sublayer on the sea floor (Chriss and Caldwell, 1982) found values smaller than 0.0025. On the other hand, measurements of the Reynolds stresses in the deep boundary layer by Gross et al. (1986) generally yielded values between 0.002 and 0.003 (but with occasional large departures).

Following the launch of TOPEX/POSEIDON, altimetry data were combined with global solutions of the Laplace tide equations, and the BBL dissipation was derived for the tidal constituents by summing $0.0025\rho\langle u_{\text{tidal}}^3\rangle$ over the globe. The final dissipation sum depends almost entirely on contributions from shallow seas. The overall accuracy is tested by comparing the astronomical total to the independently computed global work by the Moon on the ocean, which depends almost entirely on the open sea contributions. Kantha et al. (1995) compute 2.6 TW of global M_2 work as compared to the astronomically derived 2.50 ± 0.05 TW.

Newer estimates have led to somewhat reduced values for the BBL dissipation. Egbert (1997) has applied inverse methods to compute a preliminary tidal flux divergence, and he estimates 1.8 TW of BBL dissipation (M_2 only), leaving 0.6 TW for other M_2 barotropic energy losses. This value is extrapolated to 0.9 TW of total barotropic tidal losses, as compared to 0.6 TW estimated by Kantha and Tierney (1997). Some of this energy is converted into baroclinic tides, and some is available for direct and immediate turbulent dissipation. All these estimates remain very uncertain.

5.2. *Internal tides*

Internal tides with interior amplitudes of tens of meters are commonly observed. They are much too large to be generated directly by the tide producing forces. Oceanographers have long searched for scattering processes over topography for a conversion from surface to internal tidal modes (Munk, 1968; Wunsch, 1975; Hendershott, 1981).

The search was discouraged by the results of detailed calculations by Baines (1974, 1982), which gave 0.016 TW $\pm 50\%$ for 155,000 km of the global coastline. His calculations assumed a two-dimensional shelf edge. Mode conversion is proportional to Q^2, where Q is the volume flux across the continental shelf edge. But the Q-component normal to the shelf edge is generally much smaller than the flux parallel to the shelf edge. This has two important consequences: (i) transverse canyons, rills, gullies and other irregularities in the shelf edge, which had been neglected in the two-dimensional step representation, may be important scatterers (Hotchkiss and Wunsch, 1982; Thorpe, 1996; Petrunncio, 1996; Cummins and Oey, 1997), and (ii) offshore ridges, which do not constrain the flux of barotropic tidal energy, are more favorably situated with regard to energy conversion. A glance at global co-tidal charts indicates that this is the usual configuration.

Morozov (1995) produced a very large estimate for the conversion rate of barotropic to baroclinic tides; his value appears to be a considerable overestimate owing to the use of the full water depth to compute the tidal mass flux (see Munk, 1997). Sjöberg and Stigebrandt (1992) calculated the conversion from barotropic to baroclinic energy using a layered model over a stepped bottom, thus discarding the

hyperbolic character of the continuously stratified equations and the resulting critical slope interactions. Estimates of conversion rate remain conflicting and uncertain.

5.3. Hawaii mode conversion

Interest in the subject of internal tides was recently revived by some unexpected observational results. Dushaw et al. (1995) found internal tide components in acoustic travel times recorded in a 1000 km tomographic triangle deployed 2000 km north–northwest of the Hawaiian Islands. The acoustic array, which has high angular resolution, detected internal tide radiation coming from the Hawaiian Ridge. The energy flux density was 180 W/m at a range of 2000 km. Soon thereafter, Ray and Mitchum (1996) convincingly confirmed the conversion from barotropic to baroclinic tide energy by the Hawaiian Ridge. Using TOPEX/POSEIDON satellite altimetry, the internal tide was easily detected along satellite ground tracks.[14] The total energy flux was estimated at 15 GW with a decay scale of 500–1000 km, consistent with the acoustic measurements to the northwest. Kantha and Tierney (1997) have used both a global model estimate of M_2 conversion and values obtained from TOPEX/POSEIDON to calculate an M_2 conversion rate of 360 GW into baroclinic waves. They extrapolate a combined semi-diurnal and diurnal conversion value of 600 GW but suggest that the result is uncertain by about a factor of two.

The rough consistency between the magnitude of energy flux into internal tides and the dissipation associated with $\kappa_{PE} = 10^{-5}$ m^2/s (Eq. (3.15)) tempts the proposal that pelagic turbulence is maintained in this manner. A possible mechanism is the conversion of surface to internal tides along bathymetric features, a subsequent nonlinear conversion of the discrete line spectrum of the internal tides into the internal wave continuum, which in turn feeds the pelagic turbulence. Munk (1997) argues that the remarkable universality (within a factor of two) of both the fields of internal waves and pelagic diffusivity calls for a more reliable source than wind energy only. The observational situation is murky (Hendry, 1977; Wunsch and Webb, 1979). There is a large, but incomplete, literature on the nonlinear interaction of the internal tides with the ambient internal wave field (e.g., D'Asaro, 1991).

5.4. Tidal flux budget

We now return to Fig. 4. Accepting Egbert's M_2 estimate, a total (lunar plus solar) of 0.9 TW barotropic tidal energy is lost over deep sea ridges. Of this, 0.2 to 0.6 TW are radiated as internal tides and may be a major source of pelagic turbulence. The remaining power could either be in the form of trapped baroclinic tidal energy, which is dissipated locally, or be associated with a direct conversion to turbulent dissipation.

[14] The detection of internal tides from satellite altimetry came as a surprise to some of the oceanographic community who had been accustomed to impose a "rigid lid" surface boundary condition on internal waves. But the known internal amplitudes of tens of meters multiplied by a density contrast $\nabla\rho/\rho$ of order 10^{-3} give the measured surface manifestation of several centimeters.

Sjöberg and Stigebrandt (1992) assume that all of the converted energy is dissipated within 1° of its region of generation. Although consistent with some inferences of Thorpe (1992, 1996), there is a conflict with the theoretical discussion of D'Asaro (1991) and the observations already alluded to of strong internal tidal motions far from the inferred generation region.

The tentative conclusion is that the available 0.9 TW is too small to account for the 2.1 TW required for maintaining the abyssal stratification. Tidal power is adequate to mix the oceans at the measured pelagic rate (associated with $\kappa_{PE} = 10^{-5}$ m^2/s) but fails by about a factor of two to account for maintenance of the abyssal stratification (associated with $\kappa_{AS} = 10^{-4}$ m^2/s). All the numbers are subject to radical revision.

6. Inference from ocean basins

Existing tidal models suggest that tidal dissipation varies strongly between different ocean basins. Here we test the hypothesis that *differences* in tidal mixing can account for the *differences* in the basin stratifications.

Fig. 5 is an attempt to interpret the astronomical and space observations on a basin scale. The procedure is to adjust a solution to the Laplace tide equations to TOPEX/POSEIDON altimetry (we are greatly indebted to Lakshmi Kantha for providing the numbers). The six ocean basins are bounded by latitudes 48°N, 0°, 40°S to correspond to the ocean compilations. The traditional BBL dissipation for each basin was computed according to $0.0025\,\rho\,\langle u^3_{\text{tidal}}\rangle$.

We have attempted an estimate less dependent on the a priori assumptions of the dissipation physics. The upper number in (Fig. 5a) in each basin box gives the work done by the Moon, computed by integrating $\langle F\,\mathrm{d}\eta/\mathrm{d}t\rangle_{\text{time}}$ over the basin, where F is the vertical component of the M_2 tidal gravitational force (known from the lunar ephemerides, e.g. Cartwright and Edden 1973), and η is the corresponding surface elevation, which is well determined from TOPEX/POSEIDON altimetry and only weakly model dependent. As previously noted, the global sum of 2570 GW (2400 GW oceans only) is in excellent agreement with the 2500 ± 50 GW independently determined from astronomical measurements.

If the basins were enclosed, then the dissipation in each basin would equal the lunar work so determined. But we must allow for fluxes across the basin boundaries, as

Fig. 5. (a) M_2 tidal dissipation derived from tidal theory and TOPEX/-POSEIDON altimetry according to Kantha and Tierney (1997). Basin boundaries are shown and correspond to the boundaries in Fig. 6. For example, the working of the Moon on the North Atlantic (south of 48°N produces 71 GW. Allowing for the energy inflow and outflow across boundaries produces 71 + 644 − 501 = 214 GW available for dissipation. This value issmaller than Kantha's independent estimate of 362 GW of dissipation in the bottom boundary layers (BBL) of the North Atlantic. (The BBL dissipation north of 48°N totals 305 GW, including 118 GW in the North Sea and 88 GW in Hudson Bay.) The combined North and South Atlantic plus adjoining Southern Ocean sector dissipates 1050 GW, of which 902 GW is ascribed to BBL. The Atlantic sector of the Southern Ocean gains 104 GW from the Indian Ocean and 98 GW from the Pacific Ocean. (b) Dissipation for combined lunar and solar tides from Kantha (1998).

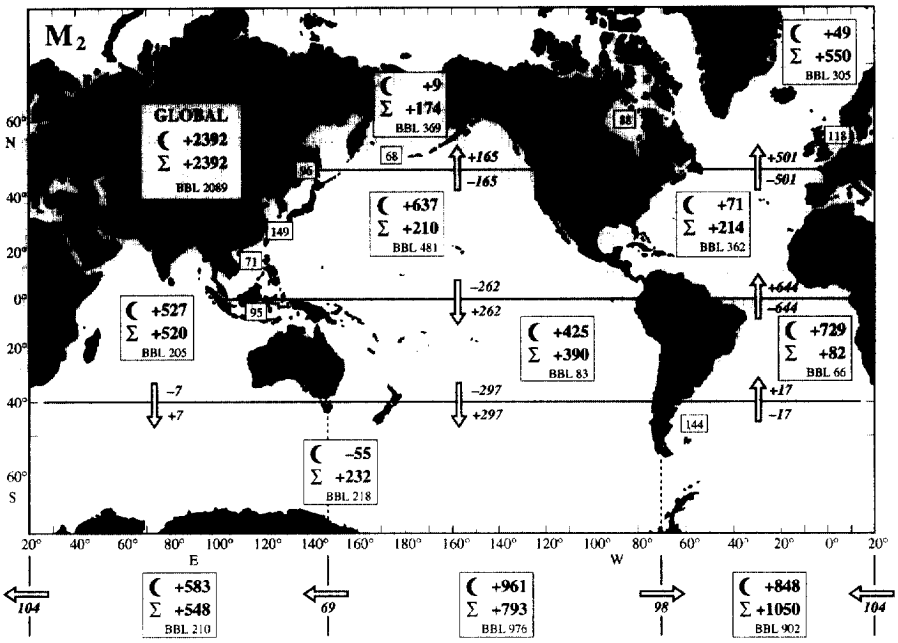
M2
GLOBAL
☾ +2392
Σ +2392
BBL 2089
☾ +9
Σ +174
BBL 369
☾ +49
Σ +550
BBL 305
☾ +637
Σ +210
BBL 481
☾ +71
Σ +214
BBL 362
☾ +527
Σ +520
BBL 205
☾ +425
Σ +390
BBL 83
☾ +729
Σ +82
BBL 66
☾ −55
Σ +232
BBL 218
☾ +583
Σ +548
BBL 210
☾ +961
Σ +793
BBL 976
☾ +848
Σ +1050
BBL 902
+165
−165
+501
−501
−262
+262
+644
−644
−7
+7
−297
+297
+17
−17
68
88
118
36
149
71
95
144
104
69
98
104
60° N
40°
20°
0°
20°
40°
60° S
20° 40° 60° 80° 100° 120° 140° 160° 180° 160° 140° 120° 100° 80° 60° 40° 20° 0° 20°
E
W

(a)

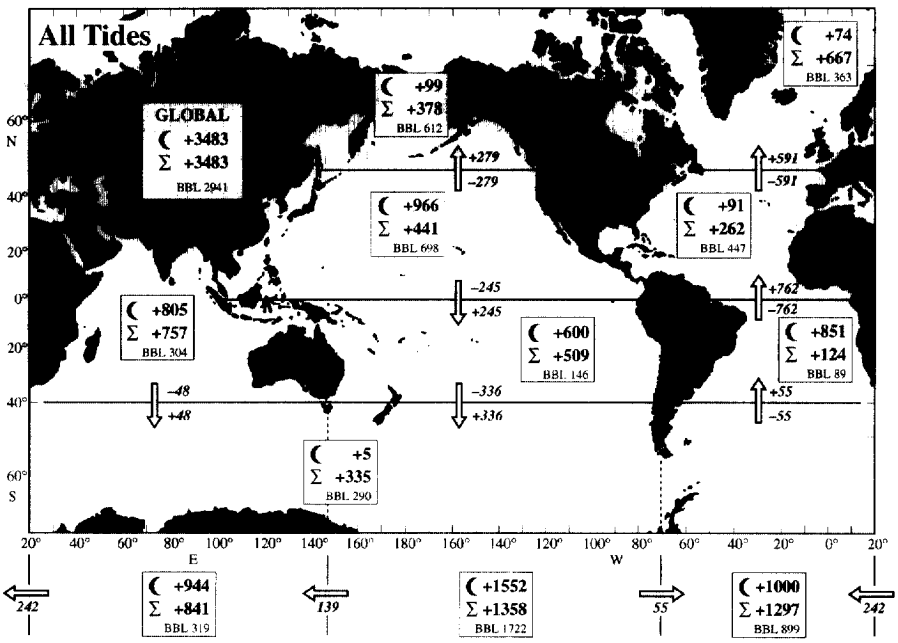
All Tides
GLOBAL
☾ +3483
Σ +3483
BBL 2941
☾ +99
Σ +378
BBL 612
☾ +74
Σ +667
BBL 363
☾ +966
Σ +441
BBL 698
☾ +91
Σ +262
BBL 447
☾ +805
Σ +757
BBL 304
☾ +600
Σ +509
BBL 146
☾ +851
Σ +124
BBL 89
☾ +5
Σ +335
BBL 290
☾ +944
Σ +841
BBL 319
☾ +1552
Σ +1358
BBL 1722
☾ +1000
Σ +1297
BBL 899
+279
−279
+591
−591
−245
+245
+762
−762
−48
+48
−336
+336
+55
−55
242
139
55
242
60° N
40°
20°
0°
20°
40°
60° S
20° 40° 60° 80° 100° 120° 140° 160° 180° 160° 140° 120° 100° 80° 60° 40° 20° 0° 20°
E
W

(b)

shown, and these depend on the assumed dissipation model.[15] For the Indian Ocean, the southward flux of 48 GW across 40°S reduces the available dissipation moderately from 805 to 757 GW, and the latter number can be used with relative confidence. For the North Atlantic, on the other hand, the flux divergence of +762–591 GW dominates the lunar input of 91 GW, and so the final dissipation estimate of 262 GW, being a comparatively small difference of large numbers, is poorly determined.

We have made a parallel attempt to estimate dissipation in the various ocean basins by inference from the ocean stratification. This first attempt to relate the observational efforts over several generations by two quite separate communities is unconvincing but suggests a pattern for future work. Fig. 6 is based on the climatological density distributions and Eq. (3.16). The values of w and their uncertainties employed here are taken from the basin estimates w^* of Macdonald (1995) and Macdonald and Wunsch (1996), where w^* was defined as the net cross-isopycnal mass flux.[16] In the inversion the constraint equations were unable to separately resolve the vertical mixing and vertical velocity. Eq. (3.8) would permit an iterative solution for the mixing, but we have not thought this worthwhile. The present result is only a crude first attempt at a qualitative picture of the basin-scale dissipation.

The basin $I(z)$ curves differ considerably from the mean global relation (dashed), but the error bars (from spatial variances) are disappointingly large. The basin dissipations have been computed for the expected w (dots) and their standard deviations (not shown), setting the dissipation to zero for negative w. The density-derived dissipation in both hemispheres in the Atlantic, Pacific and Indian basins between 48° N and 40°S is $852 + 690 + 122 = 1664$ GW.

At the lower error limit we have $394 + 380 + 0 = 774$ GW. For the equivalent basins, the altimeter-derived values are $386 + 950 + 757 = 2093$ GW and $-150 + 106 + 453 = 409$ GW, before and after subtracting the BBL dissipations. Kantha's combined northern and southern dissipations (including the Southern Ocean) are $1297 + 1358 + 841 = 3496$ GW and $397 - 364 + 522 = 558$ GW, before and after BBL subtractions.

---

[15] The energy flux bears a striking (and coincidental?) resemblance to present estimates of the oceanic heat flux (e.g., Macdonald and Wunsch, 1996), with a strong northward flux in the South Atlantic, North Atlantic and North Pacific, and with a net southward flux in the combined South Pacific/Indian Ocean sectors.

[16] In the calculations shown, three types of changes were made in the w^* values: (1) All negative values were set to zero as none of them was statistically significant at one standard deviation. As seen from the previous discussion negative w are difficult to interpret in the present context. (2) Values in the Indian Ocean were reduced by one standard deviation. The initial condition for the inversion in the Indian Ocean was based upon the conventional hydrographic analysis of Toole and Warren (1993) and is now believed (Lee and Marotzke, 1997; Robbins and Toole, 1997) to produce an unrealistically strong upwelling. (3) The South Pacific Ocean values were also reduced uniformly by one standard deviation, rendering them all zero except for the deepest one (below our depth cutoff). Here the justification is only that the extremely small apparent values of $\alpha = \mathrm{d}I/\mathrm{d}z$ otherwise produce unreasonable dissipation values. Note that the deep South Pacific hydrographic coverage is extremely poor in the Levitus climatology. Because of the large number of unstable stations in the Levitus et al. (1994) compilations in the Southern Ocean, we have not attempted the calculation in that area.

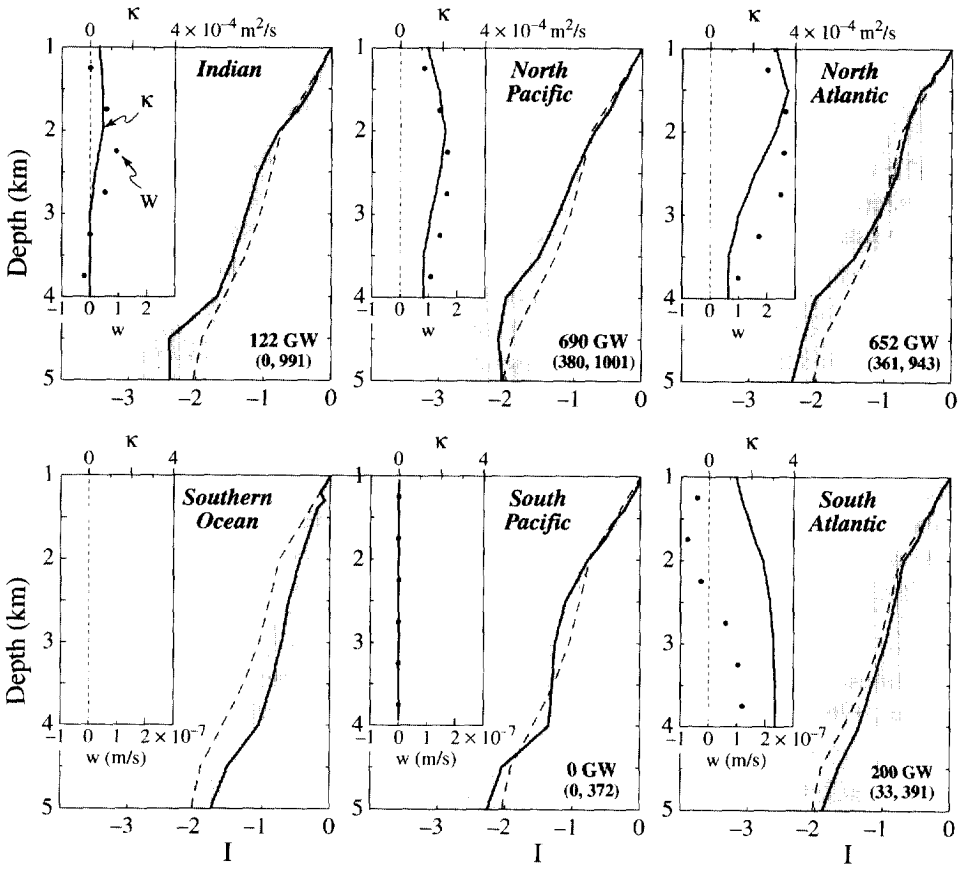

Fig. 6. Dissipation in ocean basins inferred from density distribution and vertical velocities. Solid curve with shaded band gives stability function $I(z)$ and its uncertainty; the dashed line is global mean $I(z)$ (Fig. 2). Insets give vertical velocity (dots) and diffusivity in the abyssal ocean. For comparison, the global means are $w = 0.9 \times 10^{-7}$ m/s (corresponding to 30 Sv of bottom water formation) and $\kappa_{AS} = 10^{-4}$ m^2/s (for maintaining abyssal stratification against upwelling). The abyssal dissipation in each basin is given, together with lower and upper limits corresponding to the standard deviations in $w(z)$. South Pacific w do not differ significantly from zero. Values for the Southern Ocean were not computed.

There is not much support here for the contention that tidal power maintains the abyssal stratification, other than that the density-derived and altimeter-derived dissipations are of comparable magnitude. The only positive correlation is that the dissipation densities are high in the Atlantic and low in the Pacific for both the density-derived values: 11.8 versus 4.6 mW/m^2 and the tidally-derived values: 14.4 versus 7.8 mW/m^2. This first attempt of comparing two very independent sets of observational material suffers from the large uncertainties in both datasets.

7. The wind and other energy sources

Tides and winds are the major contenders as sources of power to mix the abyss. We will not explore wind power in detail, as it would make this paper even longer, but there are some surprises worth noting.

The wind can mix the interior oceans both directly and indirectly. The *direct* route is associated with the outcrop of some (but not all) of the abyssal isopycnal surfaces in the Southern Oceans (see, for example, Fig. 2.1 of Munk et al., 1995). For the purposes of the present study we have regarded these outcrops as regions of convective injection of water masses. But to the extent that they are the site of wind-forced cross-isopycnal exchange, the interior abyssal flow can be governed by dynamical theories mentioned in the introduction, and no truly abyssal mixing is required. The interior circulation would then be that of a nearly perfect-fluid, as in the thermocline theory of Welander (1971) and its successors (e.g. Huang, 1989).

Indirect wind mixing involves the interaction of the wind-driven large-scale geostrophic motions (basin and mesoscale) with bottom topography. Another indirect mixing route involves wind-generated internal waves radiating from near the surface into the interior. Whether generated by winds or tides, the breaking of internal waves is believed to be a principal contributor to pelagic turbulence associated with $\kappa_{PE} = 10^{-5}$ m^2/s. The quantitative complexities of near-surface internal wave generation are seen in several of the papers in Müller and Henderson (1991).

Published estimates of the wind energy input into the oceanic general circulation (Faller, 1968; Fofonoff, 1981; Oort et al., 1994) are based upon the formula

$$W = \int\int_{\text{ocean}} \langle \boldsymbol{\tau} \cdot \mathbf{u}_g \rangle \, dA \tag{7.1}$$

where $\boldsymbol{\tau}$ is the windstress, $\mathbf{u}_g$ is the surface geostrophic velocity, and the bracket denotes the time average. Wunsch (1998) has made two recent recalculations, one based on a general circulation model, the other on geostrophic flow from altimetry and daily winds from the National Centers for Environmental Prediction. Both gave $W \approx 1$ TW, somewhat smaller than prior estimates and remarkably close to the tidal estimates. To close the budget in Fig. 4, we have arbitrarily assigned 1.2 TW as the wind contribution to abyssal mixing—including the generation of internal waves in the surface layer.

The buoyancy work on the general circulation was estimated by Oort et al. (1994) as 1.2 ± 0.7 TW; the error bar is very optimistic. This supports the inference that the MOC is not driven by the high latitude convective process. The MOC should not be regarded as a large-scale buoyancy driven instability; it has the appearance instead, of a partially buoyancy-forced, but stable — on the global-scale — flow. The conclusion is supported by other evidence. Bryan (1987) found that the rate of convective overturning in a GCM appeared to be proportional to $\kappa^{1/3}$, where κ is a depth-independent thermal diffusivity. The power law is dependent upon the boundary conditions and numerics employed and also on the lateral distribution of κ; Marotzke (1997) and Huang (1998b) further explore these ideas. More recently (Marotzke,

private communication, 1998) found that the intensity of the MOC in a boundary-mixed GCM was independent — over very wide limits — of the strength of the convective forcing.

8. Discussion

This paper results in many more questions than answers. Here we offer comments on (not solutions to) some of these questions.

Question 1. *Can enhanced boundary mixing, including that in canyons and along interior boundaries such as ridges and seamounts, balance the global formation of deep water in maintaining a steady abyssal stratification?*

- It seems unlikely that the regions of maximum boundary mixing have yet been found. Few abyssal measurements exist, and it is premature to estimate a global numerical average of a process dominated by a few extreme regions.
- We have shown that currents of 1 mm/s (far smaller than those associated with typical rms mesoscale circulation) are adequate to bring about a lateral homogenization spreading from mixing centers.

Question 2. *What are the candidates for the mechanical energy sources required for maintaining the abyssal stratification?*

- On the basis of the density-derived and tidally-derived numerical estimates, tidal mixing plays a *significant* but *not dominant* role in maintaining the abyssal stratification (but there is enough energy that it could *dominate* in pelagic mixing processes associated with $\kappa_{PE} = 10^{-5}$ m^2/s). Presumably winds and tides both contribute of order 1 TW to the global buoyancy flux. Both mixing processes are concentrated along special topographic features from which buoyancy (but not turbulence) is exported into the interior ocean.
- Our estimate of 2.1 TW required for maintenance of abyssal stratification could be too high by a factor of two, in which case tides alone, or winds alone, could maintain the abyssal stratification.
- Internal waves radiate into the ocean interior and are available for mixing the abyss. Some of the internal wave energy (particularly at the inertial frequency) derives from wind waves, Langmuir cells and other wind-generated surface processes (see the collection of papers in Müller and Henderson, 1991). This energy is not included in the work done against geostrophic flow.
- Wind mixing of the abyss could also occur directly through the interaction of the large-scale circulation or wind-driven mesoscale eddies with bottom topography. Indirect wind mixing could occur through the generation of mesoscale eddies from baroclinic instability of the wind-sustained available potential energy. These processes need to be quantified.
- Regions where abyssal isopycnal surfaces outcrop—particularly in the Southern Ocean—are the sites of convective injection of mass, but can also be directly

wind-mixed, thus permitting parts of the abyssal interior to be nearly adiabatic. The partitioning between surface outcrop mixing and abyssal mixing needs particular attention. High resolution measurements are required.

- Thermodynamic forcing at the sea surface is a third candidate energy source. It is the essence of Sandström's theorem that buoyancy exchange at the sea surface is an extremely inefficient generator of motion. Should the circulation be driven by the 2 PW of heat energy exchanged between ocean and atmosphere, the thermodynamic efficiency of the oceanic heat engine is extraordinarily small. Alternatively, if the circulation is primarily powered by the mechanical energy of tides and wind, the result is a heat *transport* engine of very great efficiency.

Question 3. *What is the pathway of baroclinic tidal energy generated over ridges?*

- We have referred to 0.9 TW of barotropic tidal losses over ocean ridges (Fig. 5). TOPEX/POSEIDON altimetry suggests that something like 0.2 TW are scattered into internal tides and radiated into the far field, where they could maintain the internal wave climate and ultimately the field of pelagic turbulence. In Fig. 5, we propose two pathways for the residual 0.7 TW. Thorpe (1992, 1996) finds that most of the energy converted from surface to internal tide modes over topography remains trapped in the near-field, and is locally dissipated. A second pathway involves the direct conversion of barotropic tidal energy into turbulent energy. Further progress will require a significant experimental effort.

Question 4. *Are seamounts and islands the stirring rods of the oceans?*

- It has long been known that the Bermuda slope region is one of apparent enhanced mixing (Wunsch, 1972; Gregg and Sanford, 1980). The measurements are primarily of the upper ocean on the island flanks, and no global island survey exists. The importance of island mixing in the abyss is unknown. On the other hand, Parsmar and Stigebrandt (1997) have demonstrated that sills are the stirring rods of the fjord basin water.
- Cobb Seamount (Lueck and Mudge, 1997) is a shallow seamount rising from a 3 km deep sea floor 500 km west of Washington. *Local* κ values as high as 10^{-1} m^2/s are reported; these diminish within ten kilometers to far field values of order 10^{-5} m^2/s. Current meters on the rim show energetic semidiurnal oscillations at 3 and 10 m (but not 50 m) above the rim floor. Internal tides generated at the rim propagate seaward along a refracted path extending from the rim well above the BBL and characterized by a high degree of turbulence. With measurements limited to the upper 300 m, a lower limit of dissipation is estimated at 10^7 W (R. Lueck, personal communication, 1997).

  Fieberling Guyot (Kunze and Toole, 1997) rises to a 500 m summit plane from a 4000 m abyssal plane 900 km west of San Diego. The authors interpret the dynamics as near-inertial trapped diurnal internal waves. The summit buoyancy frequency is 4.3×10^{-3} s^{-1} (2.5 cph). Fieberling has 100 km^2 of summit area. These are very similar parameters to those on Cobb Seamount, but the total dissipation is estimated as only a quarter of that at Cobb Seamount.

There are an estimated 600,000 seamounts in the Pacific, and if each would equal the Cobb dissipation of 10^7 W the total of 6 TW would exceed the upper limit imposed by the astronomical measurements. But there are many more small seamounts (with summits at small N^2) than those reaching to near the surface (Smith and Sandwell, 1997); allowing for the height distribution the dissipation is reduced dramatically from 6 to 10^{-2} TW (Susan Lyons, personal communication, 1997), even after making allowance that the number of large seamounts may have previously been drastically underestimated (Wessel and Lyons, 1997).

Question 5. *What is the connection between the strength of the convectively driven elements of the ocean circulation and the rate at which it mixes?*

- The energetics of the oceanic transport of heat (and of all the other properties important in climate such as fresh water and carbon) are seen to be intricately and remarkably bound up with the details of small scale mixing and the availability of mechanical mixing sources. The present ocean carries a meridional heat flux of about 2 PW at mid-latitudes, roughly comparable to that of the atmosphere. Is this value in some sense a saturation (a maximum) dictated by the magnitude of the tidal dissipation? Or is it controlled through direct air-sea interaction?

Question 6. *Would the general circulation of the ocean be qualitatively different if Earth had no Moon?*

Question 7. *What are the implications for the ocean stratification and heat budget in the geologic past?*

- An important role by topography in mixing, whether tidal or wind-driven, has severe implications for the ocean density distribution and circulation tens of millions of years ago when continents and mid-ocean ridges were in significantly different configurations. An important lunar role has severe implications 1 billion years ago and earlier, when the Moon was much closer to the earth.

Question 8. *How reliable is the estimate $\gamma = 0.2$, which governs the efficiency of mixing by turbulence?*

- Stigebrandt and Aure (1989) derive much lower mixing ratios ($\gamma = 0.05$) in a salt-stabilized fjord, suggesting perhaps a dependence of γ on the Prandtl number or the ambient flow.

Acknowledgements

W.M. holds the Secretary of the Navy Chair in Oceanography. C.W. acknowledges partial support by NSF Grant 9529545. We thank A. Gargett, C. Garrett, R.X. Huang, L. Kantha, M. E. McIntyre, J. Marotzke, J. Marshall, P. Worcester and W. Young for comments. Contribution to the World Ocean Circulation Experiment.

Appendix A: Solution for layered ocean

We take the case of a layered ocean with constant w and α (but not κ) within each of the layers. (We set $\kappa = 0$ in layers of negative w.) Take $h = 500$ m layers between $z_1 = -4000$ m, $z_2 = -3500$ m, ..., $z_7 = -1000$ m. From the measured density distribution $\rho(z)$, we estimate $I_i = \ln[\rho'(z_i)/\rho'_0]$ at each of the seven layer boundaries z_i (in Fig. 3, ρ'_0 is arbitrarily referred to the upper layer $z_7 = -1$ km, so that $I_7 = 0$). All subsequent integrations (upwards from z_1) depend solely upon these seven I_i values, plus the assumed six layer values of w_i. Then with $\alpha_i = (I_{i+1} - I_i)/h$ denoting the (constant) value of α between z_i and z_{i+1},

$$I(z) = I_i + \alpha_i(z - z_i), \quad z_i \leqslant z \leqslant z_{i+1}. \tag{A.1}$$

Then with $N^2(z) = N_0^2\, \mathrm{e}^{I(z)}$ and $N_i^2 = N_0^2\, \mathrm{e}^{I_i}$,

$$N^2(z) = N_i^2\, \mathrm{e}^{\alpha_i(z - z_i)}, \quad z_i \leqslant z \leqslant z_{i+1} \tag{A.2}$$

with N_0 again referring to $z_7 = -1$ km. For constant w and α

$$\kappa(z) = (w_i/\alpha_i) + (\kappa_i - w_i/\alpha_i)\, \mathrm{e}^{-\alpha_i(z - z_i)}, \quad z_i \leqslant z \leqslant z_{i+1} \tag{A.3}$$

satisfies Eq. (3.11) in layer i. The net change in diffusivity across layer i is given by

$$\kappa_{i+1} - \kappa_i = [(w_i/\alpha_i) - \kappa_i]\,[1 - \mathrm{e}^{-\alpha_i h}],$$

The diffusivities are computed starting with κ_i at the lower boundary (designated κ_0 in the text). The dissipation *density* within layer i is

$$\kappa(z)N^2(z) = N_i^2[\kappa_i - (w_i/\alpha_i)\,(1 - e^{\alpha_i(z - z_i)})]\ \mathrm{W/kg}$$

and the *total* layer dissipation is given by

$$D_i = \rho\, \gamma^{-1} N_i^2\, \alpha_i^{-1}[\kappa_i \alpha_i h - (w_i/\alpha_i)(\alpha_i h - e^{\alpha_i h})]\ \mathrm{W/m^2}. \tag{A.4}$$

Fig. 2 shows $\kappa(z)$ for two cases: $\kappa_1 = 0$ and $\kappa_1 = w_1/\alpha_1$ at $z_1(-4$ km). For the first case the condition (3.10) that $\alpha = (w - \kappa')/\kappa$ is satisfied by $w - \kappa' = \varepsilon \ll 1$ and $\kappa \approx \varepsilon/\alpha$, for the second case $\kappa' = \varepsilon w$ and $\kappa \approx w/\alpha$. For the global ocean we have the "measured" values

$$z_7 = -1\,\mathrm{km}, \quad N = 2.55 \times 10^{-3}\ \mathrm{s}^{-1}\ (1.46\ \mathrm{cph})$$

$$z_1 = -4\,\mathrm{km}, \quad N = 1.15 \times 10^{-3}\ \mathrm{s}^{-1}\ (0.66\ \mathrm{cph}).$$

Appendix B: Solution for lateral boundary[17]

We require the solution of

$$y_{zz} - \alpha y_z - \beta y_x = 0\ (x > 0,\ z < 0) \tag{B.1}$$

[17] We are indebted to John Miles for this solution.

for

$$y = y(x,z) = \frac{\rho_{-\infty} - \rho(x,z)}{\rho_{-\infty} - \rho_0} = 1 - r(x,z), \tag{B.2}$$

subject to the conditions

$$y(0,z) = e^{\alpha_0 z}\ (\alpha_0 > 0),\ y(x,0) = 1 \tag{B.3}$$

and a null condition at $z = -\infty$. Here

$$\alpha = \frac{\omega}{\kappa_{PE}},\quad \beta = \frac{u}{\kappa_{PE}}. \tag{B.4}$$

Invoking the Laplace transformation

$$\bar{y}(p,z) = \int_0^\infty e^{-px} y(x,z)\,dx, \tag{B.5}$$

we obtain

$$\bar{y}_{zz} - \alpha\bar{y}_z - \beta p\bar{y} = -\beta e^{\alpha_0 z},\quad \alpha_0 = |w|/\kappa_0 \tag{B.6}$$

and

$$\bar{y}(p,0) = 1/p, \tag{B.7}$$

the solution of which yields

$$\bar{y}(p,z) = \frac{e^{-\alpha_0|z|}}{p+\gamma} + \left(\frac{1}{p} - \frac{1}{p+\gamma}\right)\exp\{-\sqrt{\beta}|z|[\delta + (p+\delta^2)^{1/2}]\}, \tag{B.8}$$

where

$$\gamma \equiv \frac{\alpha_0(\alpha - \alpha_0)}{\beta},\quad \delta = \frac{\alpha}{2\sqrt{\beta}}. \tag{B.9}$$

The inversion of the first term in Eq. (6) is elementary; that of the remaining terms may be expressed in closed form with the aid of entry 819 in Campbell and Foster's (1942) tables. The end result is

$$y = e^{-\gamma x - \alpha_0|z|} + e^{-(1/2)\alpha|z|}\{g(|\alpha|) + g(-|\alpha|) - e^{-\gamma x}[g(|\alpha - 2\alpha_0|) + g(-|\alpha - 2\alpha_0|)]\}, \tag{B.10}$$

where

$$g(|\alpha|) = \tfrac{1}{2}\exp(\tfrac{1}{2}|\alpha||z|)\,\mathrm{erfc}[\tfrac{1}{2}|z|\sqrt{\beta/x} + \tfrac{1}{2}|\alpha|\sqrt{x/\beta}], \tag{B.11}$$

and

$$\mathrm{erfc}(\chi) = 2\pi^{-(1/2)}\int_\chi^\infty e^{-t^2}\,dt \tag{B.12}$$

is the complementary error function. We remark that Eq. (B.10) reduces to Eq. (B.3a) for all x if $\alpha = \alpha_0$ ($\gamma = 0$).

Fig. 7 is drawn for $w = 10^{-7}$ m/s (36 Sv), and $u = 1$ mm/s. The field is sharply divided along

$$x = (u/w)(\kappa_0/\kappa_{PE})(-z) = (10^{-3}/10^{-7})(10^{-4}/10^{-5})(-z) = 10^5(-z) \tag{B.13}$$

which equals 100,000 km at $z = -1000$ m (dashed line).

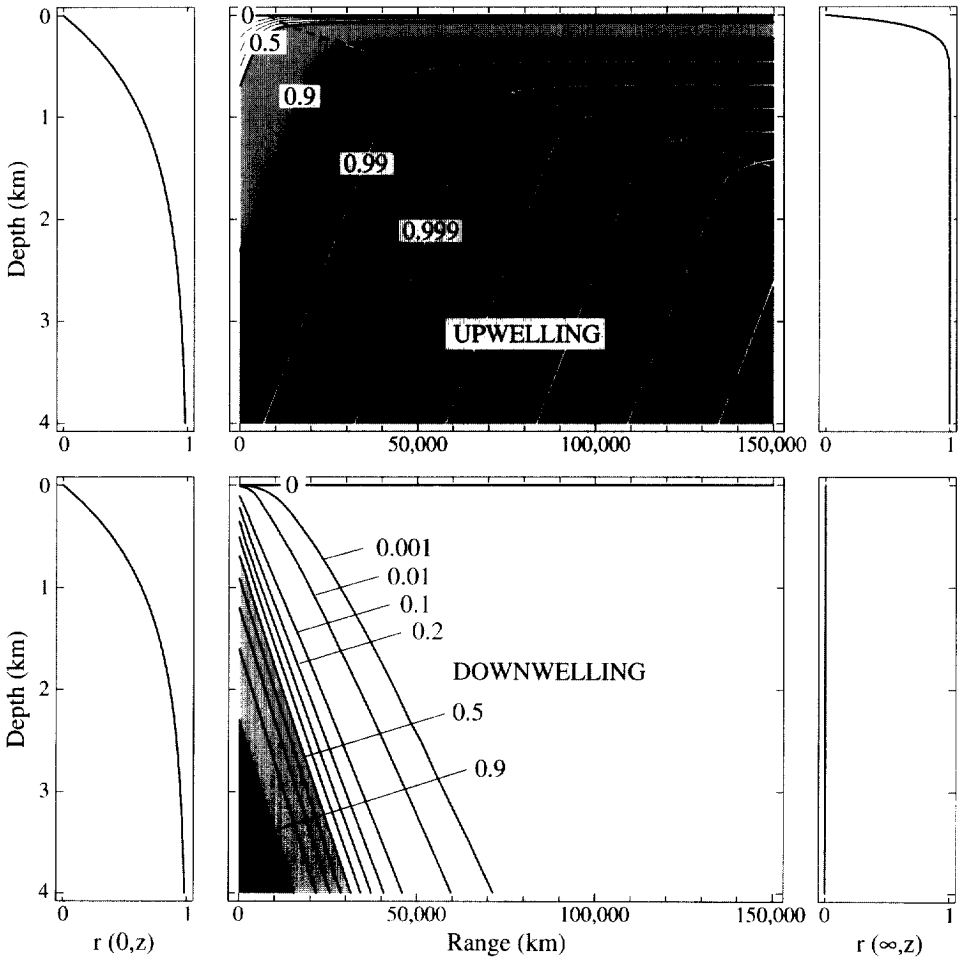

Fig. 7. The distribution of density in a convective/diffusive slice corresponding to 35 Sv globally. Contours go from $r = 0$ at the surface to $r = 1$ for bottom water. A uniform horizontal velocity of 1 mm/s in the positive x-direction is prescribed. The vertical diapycnal diffusivity is taken at 10^{-5} m^2/s. The density profile at $x = 0$ has a scale depth of 1000 m, corresponding to a diffusivity of 10^{-4} m^2/s. For the case of upwelling the vertical profile approaches the 100 m scale depth appropriate to 10^{-5} m^2/s, but only after a range of order 100,000 km. Ultimately the ocean is filled with heavy cold water (upwelling) and light warm water (downwelling).

For small x (which includes almost all the world's oceans) the solution is given simply by the first two terms in Eq. (B.10):

$$r = 1 - e^{-\gamma x + \alpha_0 z}, \quad z < 0, \quad \gamma = \alpha_0(\alpha - \alpha_0)/\beta \tag{B.14}$$

and this satisfies the differential equation (B.1) exactly:

$$\kappa \frac{\partial^2 r}{\partial z^2} - w\frac{\partial r}{\partial z} - u\frac{\partial r}{\partial x} = \kappa_{PE}\alpha_0^2 - w\alpha - u\gamma = 0. \tag{B.15}$$

It satisfies the surface boundary $r(x,0) = 0$ approximately for "short" ranges, $x < \gamma^{-1} = 10^4$ km.

We note that the isopycnals are along lines of

$$-\gamma x + \alpha_0 z = \text{constant}. \tag{B.16}$$

Appendix C: Downwelling

The non-convective downwelling example is not as geophysically absurd as one might think at first glance. Extreme volcanic activity could produce warm water bubbles that rise to the sea surface entraining water on the way (the opposite of the convective cooling at high latitudes). The global seafloor heat flux is 30 TW; about 34% or 11 TW is hydrothermal; 3 TW are associated with very young crust ($< 10^6$ yr) on the axis of mid-ocean ridges and 8 TW come from the ridge flanks ($< 50 \times 10^6$ yr) (Stein and Stein, 1994). The volume flux of interstitial water is small:

On axis: 0.003 Sv at 250°C yields 3 TW,

On flanks: 0.08 Sv at 25°C yields 8 TW.

Each liter of 350°C hydrothermal fluid entrains about 10,000 l of ambient water into a buoyant hydrothermal plume 100–300 m high and 0.025° above ambient. Allowing for entrainment, 12 Sv of vertical pumping occur along the global ocean ridge system (J. Lupton and R. Von Herzen, 1997, personal communications). R.X. Huang (1997, personal communication) has suggested that these numbers are underestimates.

Geothermal heat is a small (but not negligible) factor in the diffusive balance. One watt will heat 1 kg of sea water by $c_p = 0.24 \times 10^{-3}$°C s. W W will heat Q Sv of water formation by $Wc_p/(\rho\, 10^6 Q)$°C. Hence 30 TW will heat 25 Sverdrups by 0.25°C. This is a small amount as compared to the cooling of order 10°C associated with bottom water formation. But during periods of extreme volcanic activity the geothermal effects may be significant. Speer and Marshall (1995) show that the vertical penetration depth of even intense plumes tends to be severely limited by the effects of rotation and instabilities of the plume. Such results would confine the resulting circulation to a limited region near the seafloor. A discussion of a particular geometry is given by Thompson and Johnson (1996).

References

Alford, M., Pinkel, R., 1999. Observations of overturning in the thermocline: the context of ocean mixing. Journal of Physical Oceanography, in press.

Armi, L., 1978. Some evidence of boundary mixing in the deep ocean. Journal of Geophysical Research 83, 1971–1979.

Armi, L., 1979. Effects of variations in eddy diffusivity on property distributions in the ocean. Journal of Marine Research 37, 515–530.

Baines, P.G., 1974. The generation of internal tides over steep continental slopes. Philosophical Transactions of the Royal Society of London A 277, 27–58.

Baines, P.G., 1982. On internal tide generation models. Deep-Sea Research 29, 307–338.

Baines, W.D., Turner, J.S., 1969. Turbulent buoyant convection from a source in a confined region. Journal of Fluid Mechanics 37, 51–80.

Bryan, F., 1987. Parameter sensitivity of primitive equation ocean general circulation models. Journal of Physical Oceanography 17, 970–985.

Campbell, G.A., Foster, R.M., 1942. Fourier Integrals for Practical Applications. Bell Telephone System Monograph B-584.

Cartwright, D.E., Edden, A.C., 1973. Corrected tables of tidal harmonics. Geophysical Journal of the Royal Astronomical Society 33, 253–264.

Chriss, T.M., Caldwell, R.D., 1982. Evidence of the influences of form drag on boundary layer flow. Journal of Geophysical Research 87, 4148–4154.

Colin de Verdière, A., 1993. On the oceanic thermohaline circulation. In: Willebrand, J., Anderson, D.L.T. (Eds.), Modelling Oceanic Climate Interactions. Springer, Berlin, pp. 151–184.

Cummins, P.F., Oey, L.-Y., 1997. Simulation of barotropic and baroclinic tides off northern British Columbia. Journal of Physical Oceanography 27, 762–781.

D'Asaro, E., 1991. A strategy for investigating and modeling internal wave sources and sinks. In: Müller, P., Henderson, D. (Eds.), Dynamics of Oceanic Internal Gravity Waves, Proceedings of the 'Aha Huliko'o Hawaiian Winter Workshop. U. Hawaii at Manoa, 15–18 January 1991, pp. 451–466.

Davis, R., 1994a. Diapycnal mixing in the ocean: equations for large-scale budgets. Journal of Physical Oceanography 24, 777–800.

Davis, R., 1994b. Diapycnal mixing in the ocean: the Osborn–Cox model. Journal of Physical Oceanography 24, 2560–2576.

Dickey, J.O., Bender, P.L., Faller, J.E., Newhal, X.X., Ricklet, R.J., Ries, J.G., Shelves, P.J., Veillet, C., Whipple, A.L., Wiant, J.R., Williams, J.G., Yoder, C.F., 1994. Lunar laser ranging: a continuing legacy of the Apollo program. Science 265, 482–490.

Dushaw, B.D., Cornuelle, B.D., Worcester, P.F., Howe, B.M., Luther, D.S., 1995. Barotropic and baroclinic tides in the central North Pacific Ocean determined from long-range reciprocal acoustic transmissions. Journal of Physical Oceanography 25, 631–647.

Egbert, G.D., 1997. Tidal data inversion: interpolation and inference. Progress in Oceanography 40, 53–80.

Eriksen, C.C., 1985. Implications of ocean bottom reflection for internal wave spectra and mixing. Journal of Physical Oceanography 15, 1145–1156.

Faller, A.J., 1968. Sources of energy for the ocean circulation and a theory of the mixed layer. Proceedings of the 5th U. S. Congress of Applied Mechanics. American Society of Mechanical Engineers, held at University of Minnesota, Minneapolis, 14–17 June 1966, pp. 651–672.

Fofonoff, N.P., 1981. The Gulf stream system. In: Warren, B.A., Wunsch, C. (Eds.), Evolution of Physical Oceanography: Scientific Surveys in Honor of Henry Stommel. The MIT Press, Cambridge, MA, pp. 112–139.

Garrett, C., Gilbert, F.G., 1988. Estimates of vertical mixing by internal waves reflected off a sloping bottom. In: Nihoul, J.C.J., Jamart, B.M. (Eds.), Small-Scale Turbulence and Mixing in the Ocean. Elsevier, Amsterdam, pp. 405–423.

Garrett, C.J., 1979. Comment on 'Some evidence for boundary mixing in the deep ocean' by Lawrence Armi. Journal of Geophysical Research 84, 5095–5098.

Gregg, M.C., Sanford, T.B., 1980. Signatures of mixing from the Bermuda slope, the Sargasso Sea, and the Gulf Stream. Journal of Physical Oceanography 10, 105–127.

Gregg, M.C., 1989. Scaling turbulent dissipation in the thermocline. Journal of Geophysical Research 94, 9686–9698.

Gross, T.F., Williams III, A.J., Grant, W.D., 1986. Long-term in situ calculations of kinetic energy and Reynolds stress in a deep boundary layer. Journal of Geophysical Research 91, 8461–8469.

Hendershott, M.C., 1981. Long waves and ocean tides. In: Warren, B., Wunsch, C. (Eds.), Evolution of Physical Oceanography. Scientific Surveys in Honor of Henry Stommel. MIT Press, Cambridge, MA, pp. 292–341.

Hendry, R., 1997. Observations of the semidiurnal internal tide in the western North Atlantic Ocean. Philosophical Transactions of the Royal Society of London A 286, 1–24.

Hickey, B.M., 1997. The response of a steep-sided, narrow canyon to time-variable wind forcing. Journal of Physical Oceanography 27, 697–726.

Hogg, N., Biscaye, P., Gardner, W., Schmitz, W., 1982. On the transport and modification of Antarctic bottom water in the Vema Channel. Journal of Marine Research 40, 231–263.

Hotchkiss, F.S., Wunsch, C., 1982. Internal waves in Hudson Canyon with possible geological implications. Deep-Sea Research 29, 415–442.

Huang, R.X., 1989. On the three dimensional structure of the wind-driven circulation in the North Atlantic. Dynamics of Atmospheres and Oceans 15, 117–159.

Huang, R.X., 1998a. Mixing and energetics of the thermohaline circulation. Journal of Physical Oceanography, in press.

Huang, R.X., 1998b. On available potential energy in a Boussinesq ocean. Journal of Physical Oceanography 28, 669–678.

Jackett, D.R., McDougall, T., 1995. Minimal adjustment of hydrographic profiles to achieve static stability. Journal of Atmospheric and Oceanic Technology 12, 381–389.

Jeffreys, H., 1920. Tidal friction in shallow seas. Philosophical Transactions of the Royal Society of London A 221, p. 239.

Jeffreys, H., 1925. On fluid motions produced by differences of temperature and humidity. Quarterly Journal of the Royal Meteorological Society 51, 347–356.

Kantha, L., 1998. Tides—a modern perspective. Marine Geodesy, in press.

Kantha, L., Tierney, C., Lopez, J., Desai, S.D., Parke, M.E., Drexler, L., 1995. Barotropic tides in the global oceans from a nonlinear tidal model assimilating altimetric tides. 1. Model description and results; 2. Altimetric and geophysical implications. Journal of Geophysical Research 100(25), 283–325.

Kantha, L., Tierney, C., 1997. Global baroclinic tides. Progress in Oceanography 40, 163–178.

Killworth, P.D., 1983. Deep convection in the world ocean. Reviews of Geophysics and Space Physics 21, 1–26.

Kunze, E., Toole, J.M., 1997. Tidally-driven vorticity, diurnal shear and turbulence atop Fieberling Seamount. Journal of Physical Oceanography 27, 2663–2693.

Kunze, E., Sanford, T., 1996. Abyssal mixing: where it is not. Journal of Physical Oceanography 26, 2286–2296.

Le Provost, C., Lyard, D., 1997. Energetics of the M_2 barotropic ocean tides: an estimate of bottom friction dissipation from a hydrodynamic model. Progress in Oceanography 40, 37–52.

Ledwell, J.R., Watson, A.J., Law, C.S., 1993. Evidence for slow mixing across the pycnocline from an open-ocean tracer-release experiment. Nature 364, 701–703.

Lee, T., Marotzke, J., 1997. Inferring meriodional mass and heat transports of the Indian Ocean by fitting a general circulation model to climatological data. Journal of Geophysical Research 102, 10,585–10,602.

Levitus, S., Boyer, T.P., 1994. World Ocean Atlas 1994, vol. 4: Temperature. NOAA Atlas NESDIS 4. U.S. Government Printing Office, Washington, DC, 117 pp.

Levitus, S., Burgett, R., Boyer, T.P., 1994. World Ocean Atlas 1994, vol. 3: Salinity. NOAA Atlas NESDIS 3. U.S. Government Printing Office, Washington, DC, 99 pp.

Lueck, R.G., Mudge, T.D., 1997. Topographically induced mixing around a shallow seamount. Science 276, 1831–1833.

Macdonald, A.M., 1995. Oceanic fluxes of mass, heat and freshwater: a global estimate and perspective. Ph.D. Thesis, MIT/WHOI 326 pp.

Macdonald, A., Wunsch, C., 1996. The global ocean circulation and heat flux. Nature 382, 436–439.

Marotzke, J., 1997. Boundary mixing and the dynamics of 3-dimensional thermocline circulation. Journal of Physical Oceanography 27, 1713–1728.

Marotzke, J., Klinger, B.A., 1998. Boundary mixing and equatorially asymetric thermohaline circulation. Journal of Physical Oceanography, submitted.

McDougall, T.J., 1989. Dianeutral advection. In: Müller, P., Henderson, D. (Eds.), Parameterization of Small-scale Processes. Proceedings 'Ana Huliko'a Hawaiian Winter Workshop, pp. 289–315.

Morozov, E.G., 1995. Semidiurnal internal wave global field. Deep-Sea Research 42, 135–148.

Müller, P., Henderson, D. (Eds.), 1991. Dynamics of Oceanic Internal Gravity Waves, Proceedings of the 'Aha Huliko'a Hawaiian Winter Workshop. U. Hawaii at Manoa, 15–18 January 1991, 508 pp.

Munk, W., 1966. Abyssal recipes. Deep-Sea Research 13, 707–730.

Munk, W.H., 1968. Once again — tidal friction. Harold Jeffreys Lecture. Quarterly Journal of the Royal Astronomical Society 9, 352–375.

Munk, W.H., 1981. Internal waves and small-scale processes. In: Warren, B., Wunsch, C. (Eds.), Evolution of Physical Oceanography. Scientific Surveys in Honor of Henry Stommel. MIT Press, Cambridge, MA, pp. 264–291.

Munk, W.H., 1997. Once again: once again — tidal friction. Progress in Oceanography 40, 7–35.

Munk, W., Worcester, P., Wunsch, C., 1995. Ocean Acoustic Tomography. Cambridge University Press, Cambridge, 433pp.

Olbers, D.J., Wenzel, M., 1989. Determining diffusivities from hydrographic data by inverse methods with applications to the circumpolar current. In: Anderson, D.L.T., Willebrand, J. (Eds.), Oceanic Circulation Models. Data and Dynamics. Kluwer Academic Publishers, Dordrecht, 605 pp.

Oort, A.H., Anderson, L.A., Peixoto, J.P., 1994. Estimates of the energy cycle of the oceans. Journal of Geophysical Research 99, 7665–7688.

Osborn, T.R., Cox, C.S., 1972. Oceanic fine structure. Geophysical Fluid Dynamics 3, 321–345.

Osborn, T.R., 1980. Estimates of the local rate of vertical diffusion from dissipation measurements. Journal of Physical Oceanography 10, 83–89.

Parsmar, R., Stigebrandt, A., 1997. Observed damping of barotropic seiches through baroclinic wave drag in the Gullmar Fjord. Journal of Physical Oceanography 27, 849–857.

Pedlosky, J., 1979. Geophysical Fluid Dynamics. Springer, New York, 624 pp.

Pedlosky, J., 1996. Ocean Circulation Theory. Springer, Berlin, 453 pp.

Peixoto, J.P., Oort, A.H., 1992. Physics of Climate. American Institute of Physics, New York, 520 pp.

Petruncio, E.T., 1996. Observations and modeling of the internal tides in a submarine canyon. Ph.D. Dissertation, Naval Postgraduate School Monterey, 181 pp.

Polzin, K.L., Toole, J.M., Schmitt, R.H., 1995. Finescale parameterizations of turbulent dissipation. Journal of Physical Oceanography 25, 306–328.

Polzin, K.L., Toole, J.M., Ledwell, J.R., Schmitt, R.W., 1997. Spatial variability of turbulent mixing in the abyssal ocean. Science 276, 93–96.

Ray, R.D., Mitchum, G.T., 1996. Surface manifestation of internal tides generated near Hawaii. Geophysical Research Letters 23, 2101–2104.

Robbins, P., Toole, J., 1997. The dissolved silica budget as a constraint on the meridional overturning circulation in the Indian Ocean. Deep-Sea Research I 44, 879–906.

Samelson, R.M., Vallis, G.K., 1997. Large-scale circulation with small diapycnal diffusion: the two-thermocline limit. Journal of Marine Research 55, 223–275.

Sandström, J.W., 1908. Dynamische Versuche mit Meerwasser. Annals in Hydrodynamic Marine Meteorology, p. 6.

Schiff, L.I., 1966. Lateral boundary mixing in a simple model of ocean convection. Deep-Sea Research 13, 621–626.

Sjöberg, B., Stigebrandt, A., 1992. Computation of the geographical distribution of the energy flux to mixing processes via internal tides and the associated vertical circulation in the oceans. Deep-Sea Research 39, 269–291.

Smith, D.K., Sandwell, D., 1997. Global sea floor topography from satellite altimetry and ship depth soundings. Science 277, 1956–1962.

Speer, K.G., Marshall, J., 1995. The growth of convective plumes at seafloor hot springs. Journal of Marine Research 53, 1025–1027.

Stein, C.A., Stein, S., 1994. Constraints on hydrothermal heat flux through the oceanic lithosphere from global heat flow. Journal of Geophysical Research 99, 3081–3095.

Stigebrandt, A., 1979. Observational evidence for vertical diffusion driven by internal waves of tidal origin in the Oslo fjord. Journal of Physical Oceanography 9, 435–926.

Stigebrandt, A., Aure, J., 1989. On vertical mixing in the basin waters of Fjords. Journal of Physical Oceanography 19, 917–926.

Stommel, H., Arons, A.B., 1960. On the abyssal circulation of the world ocean—II. Idealized model of the circulation pattern and amplitude in oceanic basins. Deep-Sea Research 6, 217–233.

Stommel, H., Webster, J., 1962. Some properties of thermocline equations in a subtropical gyre. Journal of Marine Research 20, 42–56.

Szoeke, R.A.de, Bennett, A.F., 1993. Microstructure fluxes across density surfaces. Journal of Physical Oceanography 23, 2254–2264.

Taylor, G.I., 1919. Tidal friction in the Irish Sea. Philosophical Transactions of the Royal Society of London A, 230, 1–93.

Thompson, L., Johnson, G.C., 1996. Abyssal currents generated by diffusion and geothermal heating over rises. Deep-Sea Research I 43, 193–211.

Thorpe, S.A., 1992. The generation of internal waves by flow over the rough topography of a continental slope. Proceedings of the Royal Society of London A 439, 115–130.
Thorpe, S.A., 1996. The cross-slope transport of momentum by internal waves generated by along-slope currents over topography. Journal of Physical Oceanography 26, 191–204.
Toole, J.M., Schmitt, R.W., Polzin, K.L., Kunze, E., 1997. Near-boundary mixing above the flanks of a midlatitude seamount. Journal of Geophysical Research 102, 947–959.
Toole, J.M., Warren, B.A., 1993. A hydrographic section across the subtropical Indian Ocean. Deep-Sea Research I 40, 1973–2020.
Welander, P., 1971. The thermocline problem. Philosophical Transactions of the Royal Society of London A 270, 69–73.
Wessel, P., Lyons, S., 1997. Distribution of large Pacific seamounts from Geosat/ERS-1: implications for the history of intraplate volcanism. Journal of Geophysical Research 102, 22,459–22,475.
Whitworth, T. III, Warren, B.A., Nowlin Jr., W.D., Rutz, S.B., Pillsbury, R.D., Moore, M.I., 1998. On the deep western boundary current in the southwest Pacific Basin. Progress in Oceanography, in press.
Wunsch, C., 1970. On oceanic boundary mixing. Deep-Sea Research 17, 293–301.
Wunsch, C., 1972. Temperature microstructure on the Bermuda slope, with application to the mean flow. Tellus 24, 350–367.
Wunsch, C., 1975. Internal tides in the ocean. Reviews of Geophysics and Space Physics 13, 167–182.
Wunsch, C., 1998. The work done by the wind on the ocean circulation. Journal of Physical Oceanography 28, 2331–2339.
Wunsch, C., Webb, S., 1979. The climatology of deep ocean internal waves. Journal of Physical Oceanography 9, 235–243.